Groundwater Fluxes in Konya Closed Basin, Turkey

ZIZAWAR WIN NAING
March, 2011

SUPERVISORS:
First Supervisor Dr. Zoltán Vekerdy
Second Supervisor Drs. Robert Becht
Advisor Mustafa Gökmen

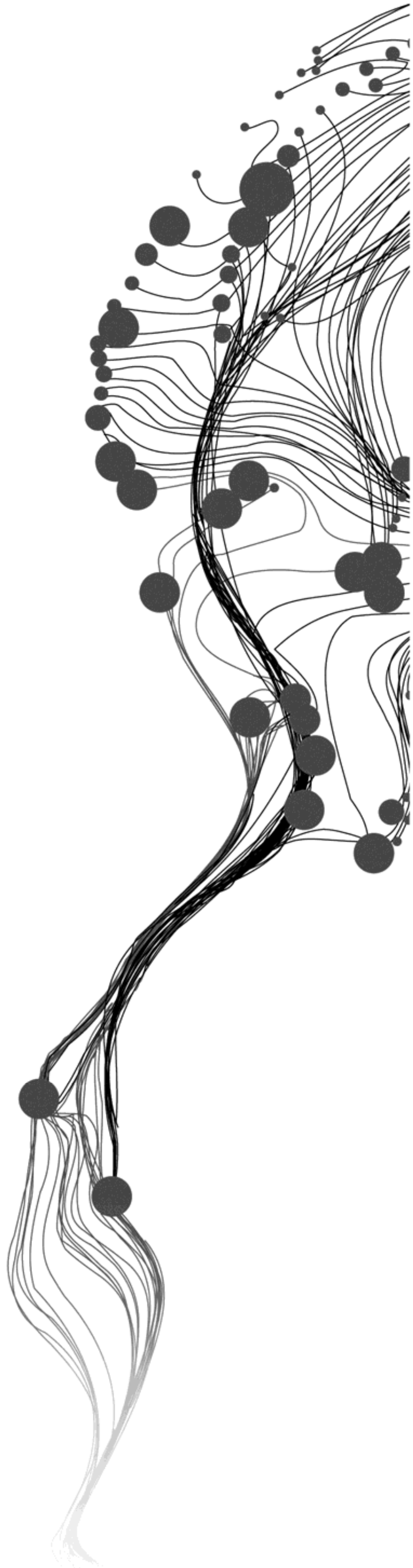

Groundwater Fluxes in Konya Closed Basin, Turkey

ZIZAWAR WIN NAING
Enschede, The Netherlands, March, 2011

Thesis submitted to the Faculty of Geo-Information Science and Earth Observation of the University of Twente in partial fulfilment of the requirements for the degree of Master of Science in Geo-information Science and Earth Observation.
Specialization: Water Resources and Environmental Management

SUPERVISORS:

First Supervisor	Dr. Zoltán Vekerdy
Second Supervisor	Drs. Robert Becht
Advisor	Mustafa Gökmen

THESIS ASSESSMENT BOARD:
Dr. Maciek Lubczynski (Chair)
Dr. Denie C.M. Augustijn (External Examiner, Faculty of Engineering Technology, University of Twente)
Dr. Zoltán Vekerdy
Drs. Robert Becht

ABSTRACT

Konya Closed Basin (KCB) is located in central Anatolia (Turkey). KCB includes Konya sub-basin in the north and Tuz Lake sub-basin in the south. The very productive karstic Neogene aquifer, reaches the maximum elevation of not more than 1150m a.s.l, with an the areal extend 51,250 km² in KCB. It outcrops in almost all of the two sub-basin areas such that groundwater can easily be accessed almost anywhere in KCB.

The objective of this study is to quantify groundwater fluxes in KCB. Moreover, to estimate accurately groundwater fluxes in a spatially distributed manner, MODFLOW-96 (Harbaugh and McDonald (1996) was applied in the karst aquifer model with a grid resolution of 5km. The map inputs include the following: recharge map based on wet season orographic rainfall, evapotranspiration map, mountain runoff. Geometry of the Neogene aquifer system was constructed in two layers according to the same hydrostratigraphic properties. The model was constructed with the target to balance the total discharge amount from the Neogne aquifer towards the Lake according to the discharge of 0.6MCM/day. In this regard, it was assumed in the model setting that all of the groundwater flow in the Neogene aquifer terminates in the Tuz Lake. Steady-state calibration of the hydraulic conductivities was carried out to obtain spatially distributed hydraulic heads. Measured hydraulic heads from hydrogeologic map (1966) were used to evaluate the steady state model calibration because the aquifer was almost at pristine state in the late 1960. By detailed analysis of the discrepancies between the measured heads and the simulated heads, an artesian area was observed since the hydraulic head was higher than the ground surface during calibration. By comparing the present time hydraulic head of Timras Sinkhole (Obruk), which is 1006 m that represents average head in 2002, the hydraulic head became 16 m lower during last 36 years. According to the groundwater budget results provided by numerical model, a total recharge of 2.2 MCM/day was found as the upper limit in steady state simulation. The model failed in quasi-transient mode due to unbalanced huge abstraction rate of 5.2 MCM/day that was adopted from two major irrigation zones: Konya Curma area and Sultanhani-Obruk-Karapina area.

The recharge of 2.2 MCM/day, which is the result of a balanced model, could not support the huge abstraction rate of 5.2 MCM/day. It was also found out that the Neogene aquifer does not balance the high evapotranspiration outflux of 7791.5 MCM/year, and the low precipitation influx with an upper limit of 2133 MCM/year. Therefore, the assumption that groundwater flow through Neogene aquifer terminates only at the Tuz Lake is not correct and there has to be other groundwater inflow/outflow components to/from the aquifer system.

If the result of head changes was possible to fit in quasi-transient mode to predict future, the head changes could represent hydrogeological environments such as lakes, wetlands and springs etc. related to the Neogene aquifer and environmental impacts could be estimated. If the head decline rate could be determined, the available groundwater reserve could be calculated and it could be estimated how long the aquifer could yield water applying the same rate of abstraction as now. Then, further calibrating the aquifer storage capacity, the ecological groundwater demand of KCB could be estimated. Therefore, the numerical groundwater modelling was found to be an important tool to estimate the spatio-temporal distribution of groundwater fluxes.

ACKNOWLEDGEMENTS

I would like to extend my deepest gratitude for the Higher Being who has been helping and guiding me all this time and especially during these tough times of thesis preparation.

I am indebted to the Erasmus Mundus Mobility for Asia Scholarship, without which my interesting experiences and pursuit of knowledge in ITC and Netherlands will not be possible.

I deeply appreciate the help and support of Lea, my dear friend and Mustafa, my adviser. Your comments, ideas, and discussions have been a big factor in the completion of this work.

I am grateful to my supervisors, Dr. Zoltán Vekerdy, for the million support, guidance and encouragement I have received, and Drs. Robert Becht, for the sound ideas in modelling.

A big appreciation for Mr. Arno van Lieshout who has been highly supportive, patient and kind.

I dedicate this work to my parents Win Naing and San San Myint, and also to Tun Tun Min, whose warmth and loving memory will forever be alive in my mind.

TABLE OF CONTENTS

LIST OF FIGURES

LIST OF TABLES

1. SCOPE OF THE STUDY

This chapter represents the background and problem statements of the research area. To improve for solving problems in the area, some objectives and research questions are followed.

1.1. Background

The role of groundwater is crucial and the only source of water supply in many arid and semi-arid region. Availability of groundwater is getting a lot of attention to balance the increasing water demand and limited water resources in all such areas. The sustainability of groundwater resources depends on hydrogeological constraints such as net recharge to the aquifers, aquifer transmissivity, aquifer storage, groundwater quality and on the anthropogenic constraints related to the human impact upon groundwater Lubczynski (2006).
The evaluation of groundwater-related fluxes such as recharge, groundwater evapotranspiration and groundwater inflow and outflow are important for the sustainable water resources management in the Konya closed basin, Turkey. Furthermore, for assessing the impacts of groundwater abstraction, the calculation of groundwater fluxes with tools, ranging from simple water balance calculations to regional groundwater models is necessary to its sustainability.
Konya closed basin (KCB), situated in the centre of Turkey, is one of the major endorheic basins in the world. The 53,000 km^2 basin is a semi-arid land where groundwater is the one of the main dependable resources. The KCB comprises northern Tuz lake and southern Konya sub-basins. Tuz Lake occupies 19% of the total area of Tuz lake basin. Taurus Mountains situated in the southern part of KCB, divide the recharge into shallow and deep groundwater flow components along the boundary between the mountain foot and the plain. These two groundwater flow components terminate at the Tuz Lake. Therefore, decreasing groundwater table could make phreatic level drop below the bottom of the lake and interrupt the groundwater flow into the lake. Since the last 3 decades, the basin has faced a hydraulic head decline in groundwater level and subsequent the shrinkage of the Tuz Lake, with high abstraction of groundwater. Moreover, the surface area of the lake is more reflective into evaporation flux, as lake shores have a little gradient. Consequently, evaporation from the lake is directly concerned with groundwater evaporation.
A detailed groundwater fluxes study in KCB can be effective for a proper management of groundwater resources.

1.2. General problem statements

Extensive usage of groundwater for irrigation since the late 1960s is threatening with groundwater head decline. Consequently declining groundwater head may cause cessation of groundwater recharge to the Tuz lake.
Bayari, Ozyurt et al.(2009) illustrated that radiocarbon age distribution of groundwater was investigated to understand the groundwater flow pattern, rate and age in the KCB. Result shows the rate of groundwater head decline about 1m/year.
Bayari, Pekkan et al.(2009) suggested about 30 m head decline of groundwater with the proof of observation in Kizoren Obruk where the groundwater exposed to 125m_deep Lake (August, 2003) compared to late the 1970.
Lubczynski (2006) elucidated that groundwater fluxes are more spatio-temporally variable and groundwater evapotranspiration is highly significant in arid and semi-arid region than in moderate climate.
Low average rainfall of 300-700mm annually occurs in the Konya closed basin on a wide areal coverage of 53,000_km^2. The low infiltration rate of overlying Quaternary aged aquitard layer which is dominant on many places in both sub basins except on Plateau, high evapotranspiration and huge groundwater abstraction in KCB are forwarding water scarcity.
Modeling groundwater flow in a karst environment is highly challenging and uncertain because of complex groundwater flow paths in the medium.

Therefore, systematic assessment of the regional groundwater flow in the KCB is critical for such a semi-arid region.

1.3. Statement of the research problem

Numerical flow models are powerful tools that allow to predict dynamic responses of aquifers related to different groundwater abstraction scenarios. An accurate physical representation of aquifers' system and suitable boundary condition are required for setting up of a reliable groundwater model. Multiple combinations of spatially dependent parameters such as aquifer thickness (D), hydraulic conductivity (K) and storativity (S) and spatially and temporally variant fluxes such as recharge (R), groundwater evapotranspiration (ETg) and groundwater inflow/outflow (Q) can lead to a non-uniqueness of groundwater model. Integration and inter-calibration of different Remote Sensing (RS) data from various sources is still a challenge to get a reasonable accuracy in evapotranspiration (ET) with time series analysis in the Konya closed basin proposed by Gökmen (2009). By introducing with spatio-temporally variant input fluxes in the time-dependent calibration in the groundwater model, more reliable solution will be provided.

1.4. Main objective

To quantify recharge and discharge components of groundwater fluxes in Konya closed basin.

1.5. Sub objectives and research questions

Specific objectives and research questions are as follows:

Specific objectives	Research Questions
1. To set up the groundwater flow model for Konya basin	Is it possible to model regional groundwater flow system in a karst environment with numerical groundwater flow modeling that is based on porous medium?
2. To determine the proper data and methods for calibration and of the model	1. Which processes and parameters can be used in the model calibration? 2. What methods can be used in model calibration?
3. To quantify groundwater budget components with groundwater flow model	Can we utilize numerical modeling method to quantify accurately groundwater fluxes spatio-temporally in the semi-arid closed basin?
4. To calibrate groundwater recharge flux	Can we determine groundwater recharge fluxes with sufficient accuracy in the semi-arid closed basin?

1.6. Research hypothesis

1. The Konya basin is hydrologically closed.

2. It is possible to model the regional groundwater system of the Konya closed basin with a Porous medium groundwater model.

2. STUDY AREA

This chapter introduce location, climate, land use, soil type, regional geology and hydrogeology of the study area.

2.1. Location

The Konya closed basin (KCB) is situated in the central Anatolian Plateau, Turkey. Its areal coverage is about 53,000 km². The study area is located between latitude 37-39° N and longitude 32-35° E and its altitude is ranging from 900m to 3000m above sea level. (Figure 2.1)

Figure 2.1. Location of the study area (source: Bayari, Ozyurt et.al(2009))

2.2. Morphology and climate

The KCB is a pear-shaped basin that comprises the southern Konya and northern Salt Lake (Tuz Golu in Turkish) sub-basins which are divided by a plateau with an approximate altitude of 1200m trending generally in east-west direction. Mean elevations of the northern and southern sub-basins are 950 and 1,100m above sea level, respectively. (Figure 3.1) The Taurus Mountain Range which rises more than 3000m at the top forms along the southern margin of the KCB basin.

The climate of the study area is arid and semi-arid region. The mean annual precipitation is about 400mm and ranging spatially between 250-800mm in the basin. Figure 2.2 Most of the precipitation occurs from October to May and in the form of snow in the mountainous areas. The climate of KCB is recognized as dry and hot in summer and moist and cold in winter generally.

2.3. Landuse

The land cover in the closed basin shows a strong contrast between intensively irrigated agricultural lands and the sparsely vegetated steppe areas covering the mid and downstream plains. Dry and irrigated agricultural lands occupy vast areas mainly in the central part of town Cumra, in the Southern part of Tuz lake, in the eastern and northern part of Beysehir lake and in the eastern part of KCB. According to the information from State Hydraulic Works, 2007, 38 % cereals, 28 % sugar beet, 19% vegetables, 13% fruits and 2 % others. Natural vegetation is dominated by Artemisia steppe Fontugne, Kuzucuoglu et al. (1999) Generally, all these step vegetation are non-woody plants with relatively short canopy height (20-40 cm) and short rooting depths. While the adaptation to the drought differs in the saline and shallow groundwater conditions in the surrounding of Tuz Lake (which are considered as wetlands), and the rest of the region, where the groundwater table is rather deep around 35 to 50 m The vegetation distribution for June 2008 is shown in Figure 2.3 based on the NDVI (Normalized Difference Vegetation Indices) extracted from MODIS satellite images in 250 m resolution.

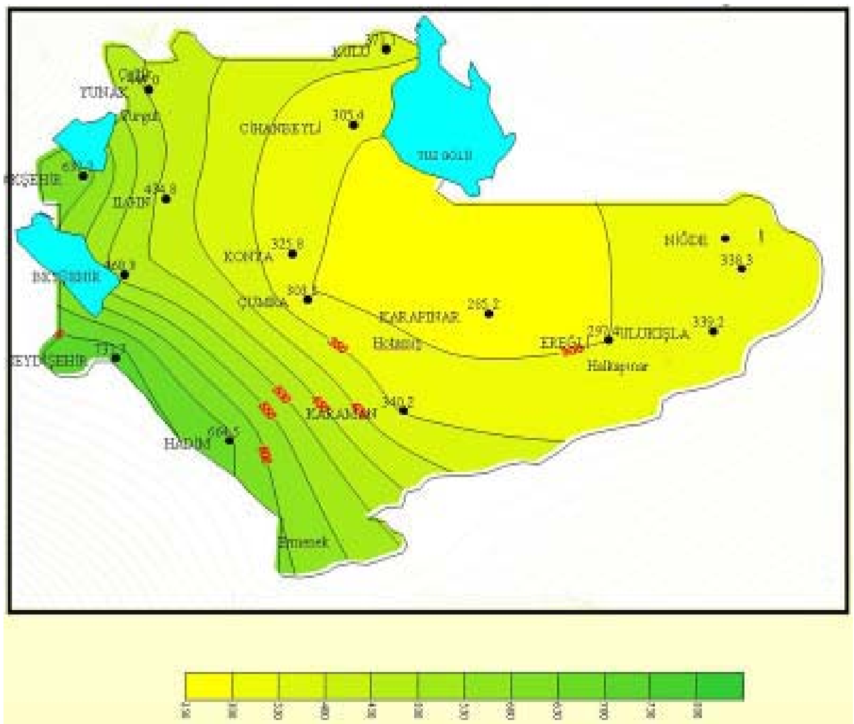

Figure 2.2. Annual rainfall distribution in Konya closed basin (source : unpublished data by DSI, Turkey)

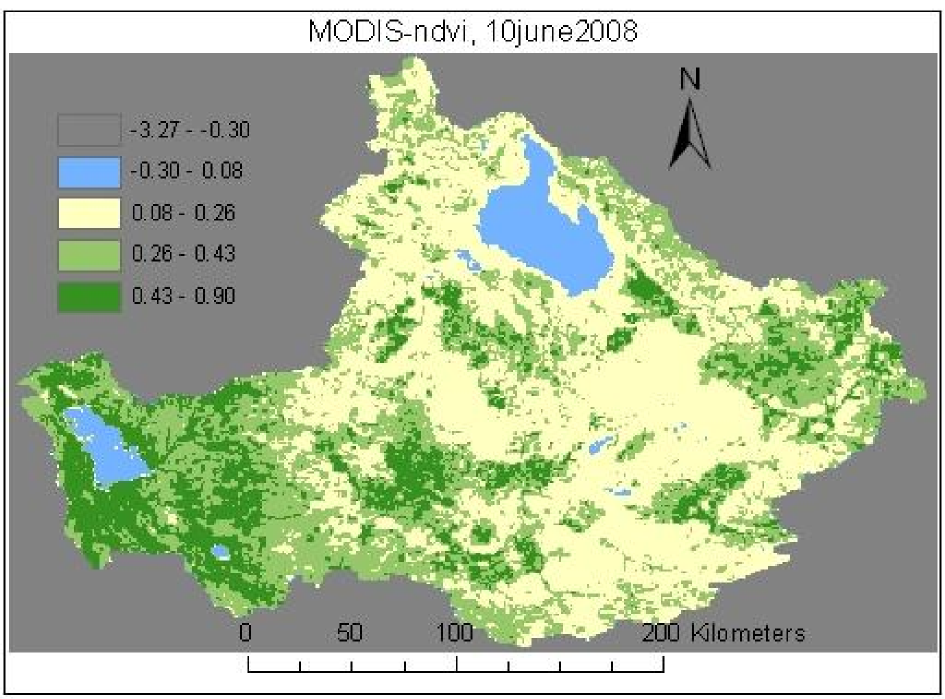

Figure 2.3. A vegetation distribution map based on NDVI (source: Gökmen (2009))

2.4. Soil type

Meester (1970) describes in detail the soils of the Konya closed basin. The Basin is tectonic and contains clastic material, which is over 300 m thick here and there and is surrounded by uplands of limestone or volcanic rock. In the Pleistocene epoch the central part was covered by a lake which has silted up, and has been drained since, except for some marshy areas like Hotamis Gölü and Ak Göl. The former lake bottom is now very flat and occupies the central part of the area. Its soils are developed from highly calcareous clay, silt or sandy loam, generally called marl.

The soils of the alluvial fans in the mountain fringes and plains have developed from calcareous clays or loams and have weakly developed profiles, usually being classified as Inceptisols. Remains of Neogene structural limestone terraces, which are almost horizontally stratified, occur at several places in the Basin, mainly south of Çumra and west of Karapinar. Their soils are derived from calcareous clay and are old enough to containa well developed calcic horizon. Most profiles are Aridisols.

2.5. Regional geology

Three lithosperic plates namely Tauride-Antolide Block (TAB), Sakarya Zone Block (SZB), and Kirsehir Massive Block (KMB) are encountered in the study area in Bayari, Ozyurt et al. (2009) . The TAB is composed of early Paleozoic to late Mesozoic rocks of clastic (conglomerates, sandstone and shale), metamorphic, ophiolitic and marine carbonate origin (dolomite, limestone and dolomitic limestone). The SZB comprises Triassic subduction-accretion complex followed by Jurassic clastics; Jurassic to Cretaceous carbonates, Middle-late Cretaceous clastics and volcanics, and ends with Paleogene carbonates and clastics. The KMB consists of metamorphic and voluminous granitic rocks of cretaceous age. Neogene with the age ranging from late Miocene to late Pliocene, starts from basal conglomerate and continue upward to lacustrine carbonates (i.e limestone and dolomite) alternating with marl in some places. The Quaternary aged paleolake sediments and alluvial fans cover vast area in both sub-basins. Figure 2.4.

The presence of numerous gigantic collapse dolines (obruks in Turkish) developed in the lacustrine Neogene carbonates and small no of obruks outcrop along the Taurus mountains' flank and large amount are along NW-SE extending trend line of middle plateau.

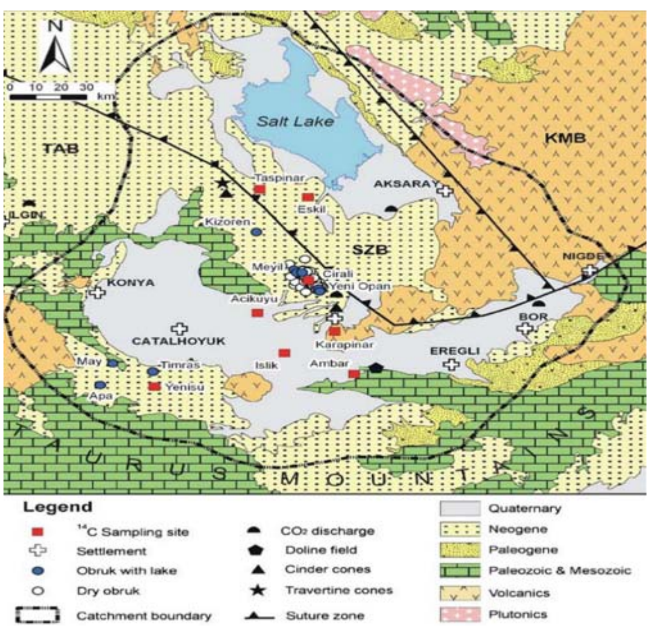

Figure 2.4.Simplified geological map of the study area (source: Bayari, Ozyurt et al. (2009))

2.6. Regional groundwater aquifer and flow system

Among all geologic units in KCB, the TAB, SZB and Neogene units represents as aquifer systems while the Paleogene and Quaternary paleolake sediment (QPS) units are aquitard systems. According to the conceptual model of cross-section of KCB, groundwater flows from the Taurus mountains in the south (main recharge area) to the Tuz Lake in the north (main discharge area). The recharge from Taurus mountains is divided into two groundwater flow components along the boundary between the mountain flank and the plain area. Regionally, these two groundwater flow components create two major aquifer system: a shallow and high productive fresh-water aquifer at the top and confined and deep thermal saline-water aquifer below. The shallow groundwater pass through the Neogene fresh-water aquifer toward the Tuz Lake in Figure 2.5. Impermeable character of QPS above the fresh-water aquifer covers throughout the southern and northern sub-basins, therefore, the fresh-water aquifer is confined in these regions. At the flank of Taurus mountains and in the middle plateau, the aquifer behaves as unconfined conditions.

An interesting hydrogeologic observation on the obruks is the distinction between NW-SE trend line of obruks plateau and the northward direction of regional groundwater flow line. This shows that the karstification is leading in the vertical direction progresses and is not lateral continuation to divert groundwater flow. Therefore, the high hydraulic conductivity zone of karstic Neogene carbonates seems to attract both the local recharge around the plateau obruks and the regional groundwater flow. Well-developed karstic features are able to be observed in the TAB and Neogene aquifers.

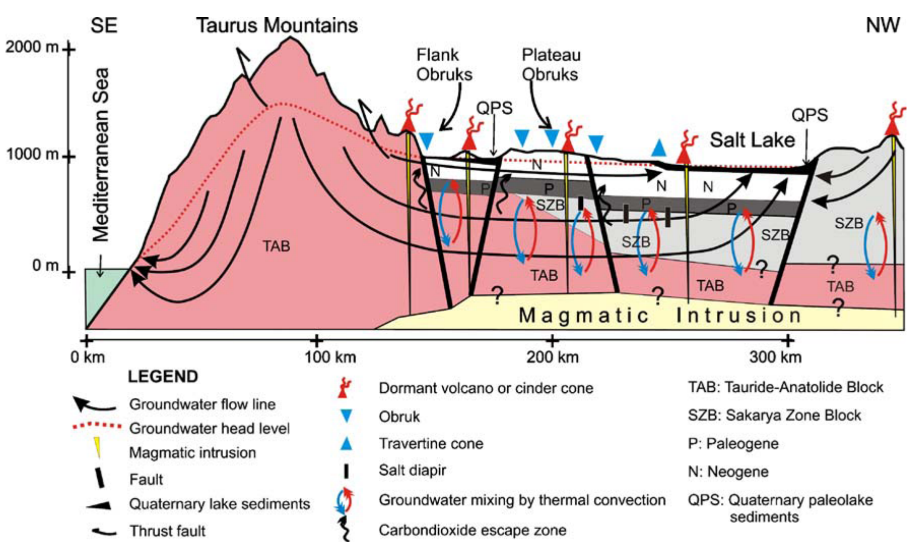

Figure 2.5.Conceptual hydrogeologic flow system (source: Bayari, Ozyurt et al.(2009))

2.7. General steps in the research study

The general steps that have to be carried out in this research study is shown in Figure 2.6.

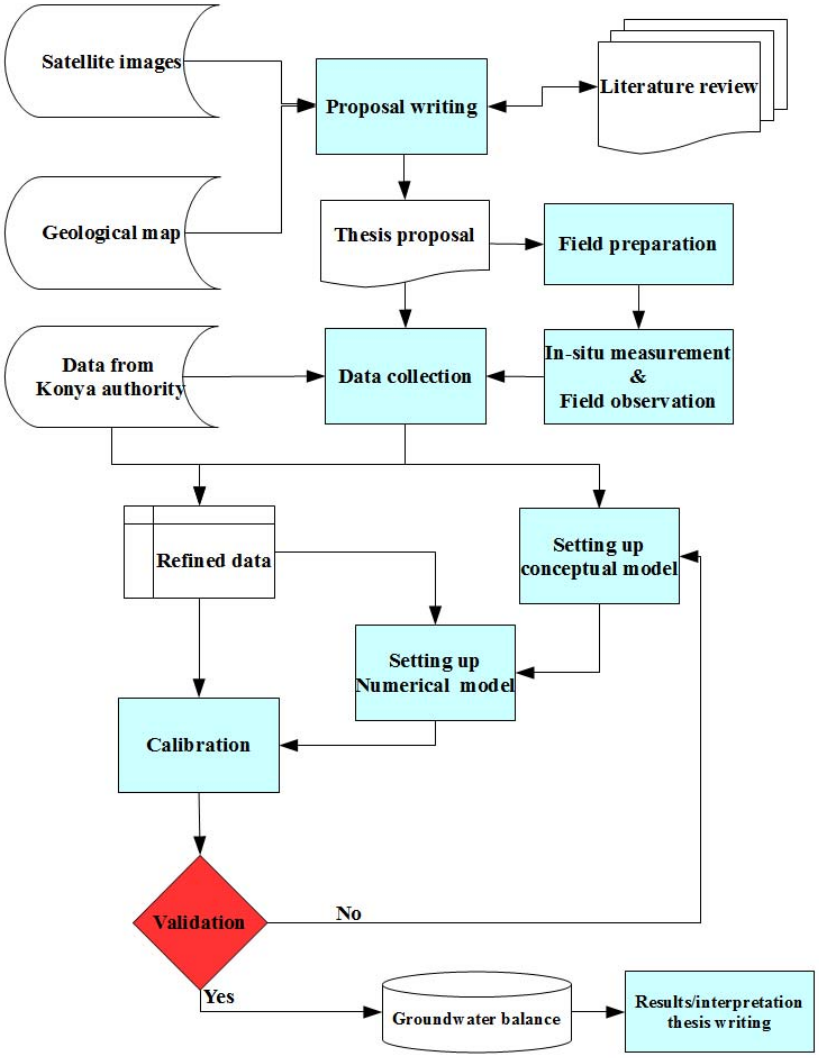

Figure 2.6. A general flow chart showing main steps in research

3. DATA INTERGRATION

This chapter is proposed to compile, process, analyse and synthesize the available primary and secondary data for parameterization and calibration of groundwater flow model. All parameters and data were prepared with the area of (51250 km²) of the Model boundary based on 5 x 5 km² pixel size. Figure 3.1

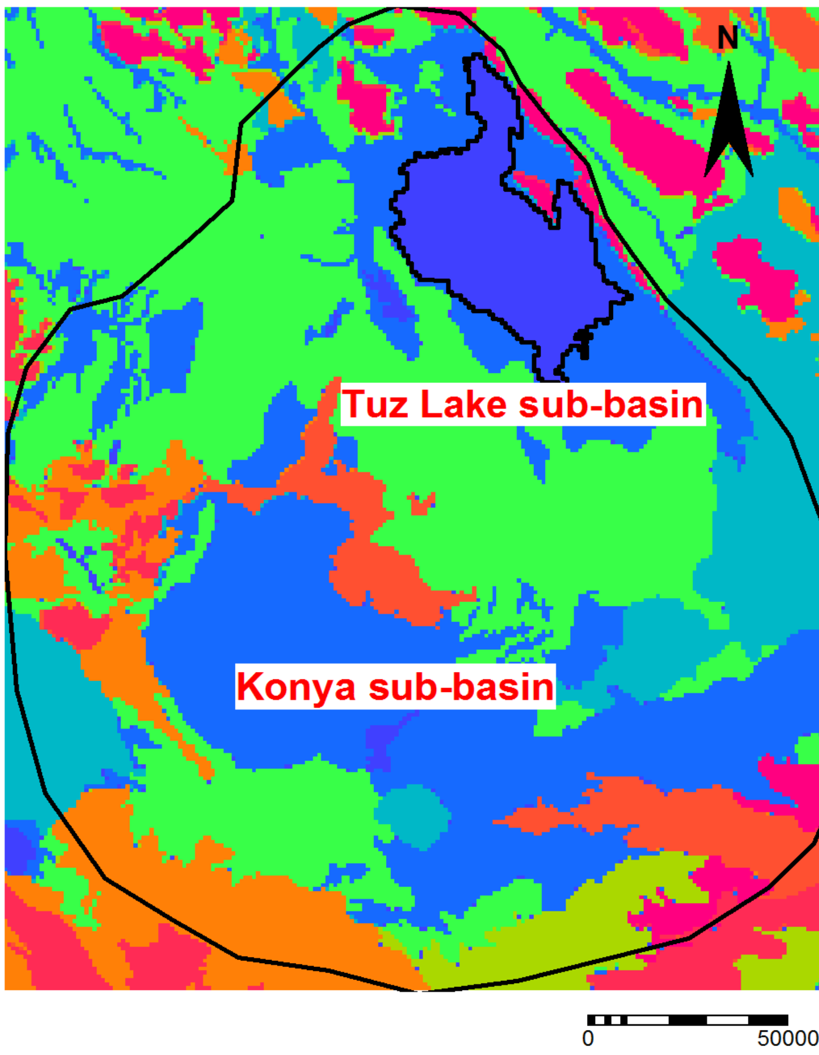

Figure 3.1. The boundary of the Model area

Main tasks on the data integration are as follows:

i. Digital elevation model(DEM)
ii. precipitation map
iii. actual evapotranspiration map
iv. recharge map
v. aquifer properties derivation from pumping tests
vi. monthly hydraulic head
vii. aquifer thickness derivation

3.1. Digital elevation model (DEM)

The SRTM DEM(82.612m resolution) was downloaded with the coverage on the research area. Filtering, resampling and aggregating were carried out to convert into 5 x 5 km^2 pixel as described in the text book Tempfli, Kerle et al.(2009).

3.2. Precipitation (P)

3.2.1. Available information

Rainfall in a semi-arid region is usually intensive if present normally occurs in shorter time and spatially and temporally variable as described in section 2.2.
Daily rainfall data of 11 stations in the KCB from 1980 to 2010 are available (Figure 3.1) Hadim, Yunak and Eregli stations are located in high-land regions about 1550 m, 150 m and 1050 m respectively. The elevation of the rest stations vary between 960-1000 m.s.a.l.

3.2.2. Material & Methods

In such a highly vary in elevation region, the precipitation can be markedly affected by topographic features, such as elevation, slope and aspect of the land surface. Brutsaert (2005) pointed the relationship between precipitation and elevation is usually more pronounced for convective rainfall caused by orographic effects according to the observation by Suzuki et.al (2002). The relationship is more apparent for larger rainfall amounts and longer time span. With monthly rainfall data, the effect of elevation is elucidated with stronger relationship than the effects of other factors. For those reasons, the method of linear relationship between monthly total rainfall data and elevation is applied to incorporate digital elevation models (DEM) to produce a precipitation map with pixel size 5 x 5 km^2. The wet season from November to May and the dry season from June to October are defined based on the annual rainfall analysis. (Figure 3.2) (Table 3.1)

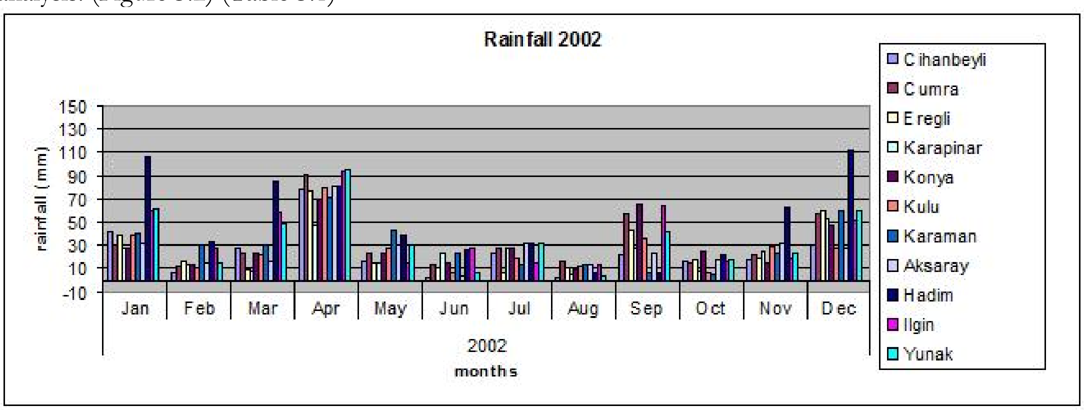

Figure 3.2. Monthly rainfall distribution from 11 meteorological stations

year	month/station name	Cihanbeyli	Cumra	Eregli	Karapinar	Konya	Kulu	Karaman	Aksaray	Hadim	Ilgin	Yunak	total monthly rainfall(mm)
2002	Jan	41.5	29.8	38.9	28.3	27.8	40	40.9	31.8	106.5	60.9	62.1	508.5
	Feb	6.9	12.1	15.8	12.8	12.9	10.2	30	14.3	33.4	27.1	15.2	190.7
	Mar	26.6	22.3	8.9	7.5	24.2	21.9	30.1	16.8	84.4	58.9	48.5	350.1
	Apr	78.7	91	77.2	47.9	70	79.3	70.7	81.7	80.1	93.6	94.9	865.1
	May	16.3	22.8	15.6	14.1	22.9	26.7	42.7	29.5	38.8	14.6	29.8	273.8
	Jun	2.9	13.2	11.3	23.3	15.3	6.6	23.9	3.4	25.6	27.3	5.4	158.2
	Jul	22.2	27.1	7.1	26.5	27.1	19.7	13.4	32.3	31.1	15.1	32.6	254.2
	Aug	2.8	16.4	10.7	4.5	8.7	11.6	13.6	12.8	6.8	13	3.8	104.7
	Sep	21.8	56.9	43.1	27.8	65.8	35.1	7.3	22.2	6.5	64.9	41.3	392.7
	Oct	16.4	14.7	17.1	8.1	24.6	6.1	4.9	17.1	21.2	16.2	17.8	164.2
	Nov	17.2	22.1	18.3	24.9	15.3	28.8	22.2	31.9	62.6	20	23.1	286.4
	Dec	30.3	57.7	60.4	53.3	48	27.3	60.1	27.9	112.5	52.3	59.3	589.1
	total (mm)	283.6	386.1	324.4	279	362.6	313.3	359.8	321.7	609.5	463.9	433.8	344.8

Table 3.1. Monthly rainfall data from 11 meteorological stations

The year 2002 which represents a average year in term of rainfall was selected for modelling. The approach consists of modelling the relationship between elevation of measured stations and the total rainfall during the wet season using a linear regression. (Figure 3.3) The relation shows 85% correlation of the two parameters. (Equation 3.1)

$$\mathbf{P_{season} = 0.5102x - 267.82} \qquad \mathbf{3.1}$$

Where

P_{season} = orographic rainfall for the wet season in mm

x= elevation in m

This relation is then applied to calculate the orographic rainfall map of the wet season. The monthly orographic rainfall amounts in the wet season were defined by division with 7 (the wet season comprises 7months). (Table 3.2)

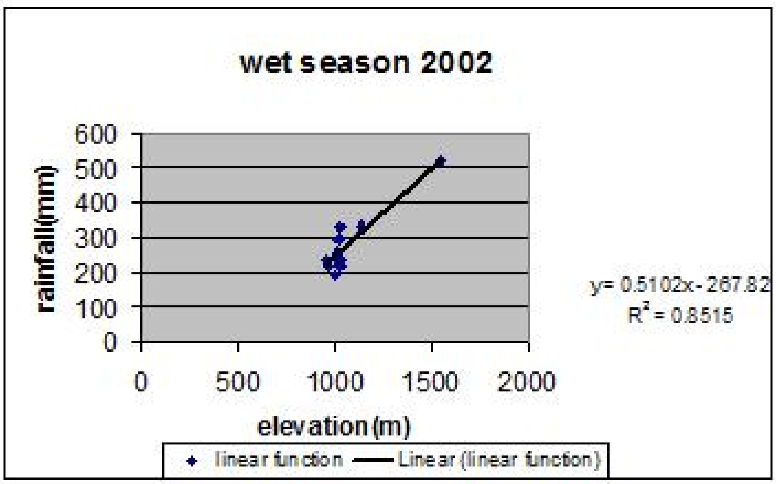

Figure 3.3.Linear relationship between elevation and rainfall

No	Station name	elevation	orographic rainfall	average orographic rainfall
1	Cihanbeyli	968.7	226.41	32.34
2	Cumra	1013	249.01	35.57
3	Eregli	1042	263.81	37.69
4	Karapinar	1004	244.42	34.92
5	Konya	1031	258.20	36.89
6	Kulu	1010	247.48	35.35
7	Karaman	1023	254.11	36.30
8	Aksaray	960.8	222.38	31.77
9	Hadim	1552	524.01	74.86
10	Ilgin	1034	259.73	37.10
11	Yunak	1140	313.81	44.83

Table 3.2. Monthly orographic rainfall amount in the wet season

There are some differences between the orographic rainfall map and measured rainfall at every station. These differences at each station are calculated on monthly basis and interpolated with 2nd order polynomial Trend surface method. The resulted monthly differences maps are added to monthly orograhic rainfall maps to get the actual rainfall maps. (Equation 3.2)

$$\mathbf{P_{month} = P_{season} / 7 + \Delta P_{month}} \qquad \mathbf{3.2}$$

Where
P_{season} = the orographic rainfall of the wet season
ΔP_{month} = the monthly difference between the orographic rainfall and the actual rainfall

For the dry season, monthly rainfall data are simply interpolated with 2nd order polynomial Trend surface method and then added to actual rainfall maps of wet season to get average annual rainfall map. (Figure 3.4)

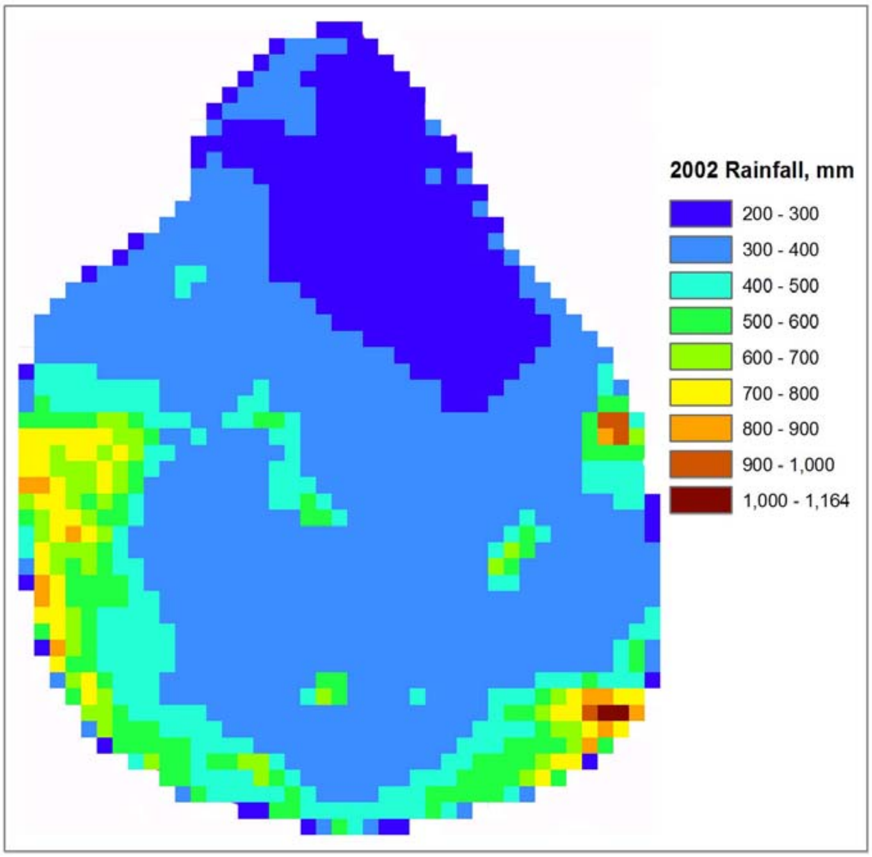

Figure 3.4. Spatial distribution of the precipitation map for the year 2002

Calculation of the total volume precipitation based on different areas is carried out according to Equation 3.3.

$$R_{tot} = \sum_{i=1}^{Npix} P_i \, A \, 1000 \qquad 3.3$$

Where
P_{tot} = volume of precipitation (million m^3, MCM)
P_i = precipitation in the pixel (mm)
$Npix$ = no of pixels
A = 25 km^2 = area of the pixel

Daily, monthly and yearly average precipitation depend on different areas are shown in (Table 3.3).

period	Plain area(MCM)	mountain area(MCM)	Tuz lake(MCM)	the model area(MCM)
			area = 1725 km^2	area = 51250km^2
Jan-02	836.81	711.14	59.99	1607.94
Feb-02	360.56	461.49	7.44	829.48
Mar-02	514.17	564.66	23.05	1101.88
Apr-02	1883.71	1026.25	124.78	3034.74
May-02	578.82	502.18	31.46	1112.46
Jun-02	303.35	193.65	8.43	505.42
Jul-02	568.20	217.40	45.44	831.04
Aug-02	242.58	105.63	16.97	365.18
Sep-02	953.75	372.44	53.13	1379.32
Oct-02	345.73	162.86	23.03	531.62
Nov-02	562.07	514.01	38.51	1114.58
Dec-02	1052.39	907.85	36.38	1996.62
total	8202.12	5739.54	468.60	14410.26
daily average	22.47	15.72	1.28	39.48

Table 3.3.Contribution of precipitation in different areas

3.2.3. Result & discussion

According to the residue result in Appendix A1, April had more rainfall than the expected orographic rainfall and Hadim station, situated on the higher elevation than other stations has the least discrepancy in this high intensity rainfall month. In opposite, February shows deficit rainfall compared to the orographic one because orographic rainfall is less effective in low rainfall months. On the whole year basis analysis, rainfall is in the range of 200_400mm in low-lying plain area. In spatial extent, the southern sub-basin receives more rainfall about 400mm/year than the northern sub-basin, about 250mm/year. On the plateau separating the two basins, about 450-500mm rainfall occurs at altitude of about 1200m. The rest of high - land area receive high rainfall about 600mm and 800mm at about 1500m and 2000m elevations respectively.

3.3. Actual evaporatranspiration(ETa)

3.3.1. Available information

Available actual evapotranspiration maps on monthly basis for year 2002 is provided by Gökmen (2009). Evapotranspiration map of year 2002 is shown in Figure 3.5.

3.3.2. Material & methods

Methods based on Surface Energy Balance System(SEBS) the work of Su (2002) using remote sensing techniques give the results of actual evapotranspiration over the KCB.
The volume of ETa on the different areas were calculated and analysed with the following Equation 3.4.

$$ET_{tot} = \sum_{i=1}^{Npix} ET_i\, A\, 1000 \qquad 3.4$$

Where
ET_{tot} = volume of evapotranspiration (MCM)
ETi = evapotranspiration in the pixel
$Npix$ = no of pixels
A = 25 km^2 = area of the pixel

The value 1000 is the unit converting factor.

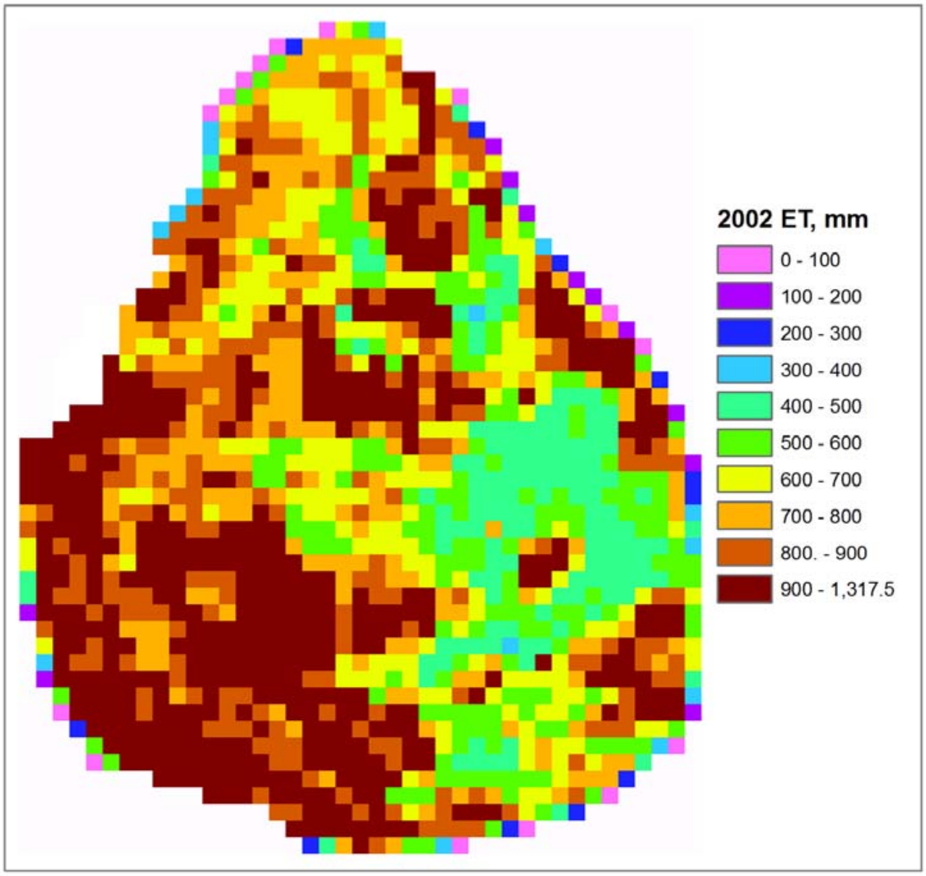

Figure 3.5.Spatial distribution of evapotranspiration map for the year 2002

Daily, monthly and yearly average evapotranspiration depend on different areas are shown in (Table 3.4).

period	mountain area(MCM)	irrigation area(MCM)	wetland area(MCM)	Tuz lake(MCM)	Plain area(MCM)	Model area(MCM)
				area = 1725 km^2		area = 51250km^2
Jan-02	183.86	115.22	3.87	19.59	279.27	601.81
Feb-02	479.88	338.35	12.72	66.16	816.02	1713.13
Mar-02	562.97	392.50	18.46	98.80	910.90	1983.63
Apr-02	730.55	563.76	18.22	87.50	1203.01	2603.04
May-02	1452.76	1239.06	37.81	194.78	2782.22	5706.62
Jun-02	1315.16	1153.75	40.65	180.79	2279.26	4969.61
Jul-02	1454.69	1269.85	46.58	188.85	2424.61	5384.58
Aug-02	1240.97	1039.46	38.46	167.04	2064.39	4550.33
Sep-02	1018.36	702.42	26.76	136.53	1599.78	3483.85
Oct-02	777.72	556.07	19.57	50.13	1337.99	2741.47
Nov-02	439.36	306.41	10.25	50.13	701.17	1507.31
Dec-02	158.89	114.64	4.88	26.41	290.98	595.80
total	9815.16	7791.50	278.21	1266.70	16689.61	16689.61
daily average	26.89	21.35	0.76	3.47	45.72	45.72

Table 3.4. Contribution of evapotranspiration in different areas

3.4. Recharge assessment

3.4.1. Available information

Monthly precipitation and actual evapotranspiration maps for year 2002 were available to estimate spatial distributed recharge. Besides the direct precipitation, some surface runoff also reaches the two low-lying basins. There are several ephemeral streams flowing to the Tuz Lake. Besides, canal was constructed in the beginning of the twentieth century to deliver water from the Beysehir Lake in the southwest towards the Tuz Lake. Nowadays little or no water reach actually the Tuz Lake as a result of interception by farmers for irrigation, clogging it with dumping waste in its bed. In the southern sub-basin, KCB has the mountain front systems such as alluvial fans, piedmont plains and subsidence basins. A mountain front recharge is expected to occur in the transition zone of the mountains to the flat plains, i.e. along the footslopes.

3.4.2. Material & methods

Available recharge over the modelled area was calculated according to the Equation 3.5 for the wet season of the year.

$$R = P - ETa \qquad when\ P > ETa \tag{3.5}$$

Where
R = recharge (mm)
P = precipitation (mm)
ETa = actual evapotranspiration (mm)

Only the wet season was taken into account to represent recharge. An assumption of no recharge in the dry season in semi-arid region is considered. When the value of evapotranspiration is larger than precipitation in each cell, the recharge was set into zero recharge is applied. To avoid underestimating available recharge for the study area, irrigation area is eliminated from evapotranspiration map and were replaced with ETa values of the surrounding natural vegetation. To account for the recharge from surface runoff along the mountain fronts of KCB, an estimated 10% runoff coefficient was applied to the mountain precipitation and was distributed as recharge along the foot slopes. The spatially distributed recharge map is shown in Figure 3.6 and the recharge at different regions is shown in Table 3.5.

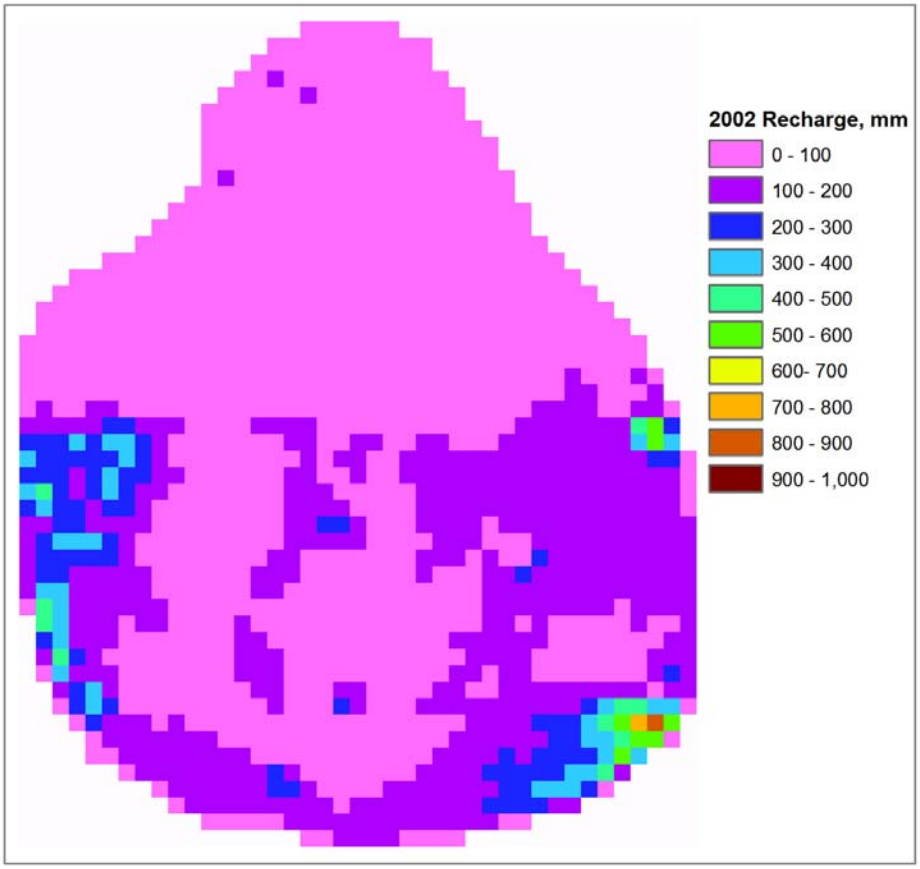

Figure 3.6. Spatial distribution of the recharge map for the year 2002

period	model area(MCM)	mountain area(MCM)	mountain runoff(MCM)	plain area(MCM)	potential recharge
			10% of mountain rain		area = 51250km^2
Jan-02	1121.35	587.27	58.73	534.08	592.81
Feb-02	92.46	82.36	8.24	10.10	18.34
Mar-02	127.80	125.12	12.51	2.68	15.19
Apr-02	1026.45	429.40	42.94	597.05	639.99
May-02	9.79	9.79	0.98	0.00	0.98
Jun-02	0.00	0.00	0.00	0.00	0.00
Jul-02	0.00	0.00	0.00	0.00	0.00
Aug-02	0.00	0.00	0.00	0.00	0.00
Sep-02	0.00	0.00	0.00	0.00	0.00
Oct-02	0.00	0.00	0.00	0.00	0.00
Nov-02	187.39	144.83	14.48	42.56	57.05
Dec-02	1515.62	785.34	78.53	730.28	808.81
total	4080.86	2164.11	216.41	1916.75	2133.16
daily average	11.18	5.93	0.59	5.25	5.84

Table 3.5. Contribution of recharge in different areas

3.4.3. Result & discussion

The resulting of potential recharge 5.84 MCM/day is upper limitation of probable recharge (i.e. can be considered as potential recharge) to the groundwater table. The actual recharge is still defined by the soil water storage according to the standard soil water balance calculation. Equation 3.6

$$Ra = P - ETa + \Delta S - Ro \tag{3.6}$$

Where,

Ra = actual recharge;

P = precipitation;

ETa= actual evapotranspiration;

ΔS = change in soil water storage; and

Ro = run-off

Therefore, no reliable information concerning absolute values of recharge can be obtained by the surface water balance. Still, the resulting difference-map (P–ETa) can be used for the identification of distinct zones of potential for recharge in water resource management.

3.5. Aquifer properties derivation from pumping test

3.5.1. Available information

Pumping test data of total (18) wells are provided by DSI (State Hydraulic Works of Turkey) .The dataset contains the pumping test data only and does not contain continous groundwater level observation. The measurement of groundwater drawdown(m) and specific time steps(min) with discharge rate are available to estimate aquifer properties. Construction material of pumped wells and graphical expression of lithologic succession are also helpful to judge an aquifer's hydraulic conductivity and transmissivity. However, estimation of aquifer storage properties from single pumped well tests is generally discouraged because those tests are affected by well bore storage that reflect the withdrawal of water stored in the casing and that well-bore storage in turn affect the early drawdown illustrated by Boonstra and Kselik (2001).

3.5.2. Material & methods

To calibrate aquifer hydraulic conductivity and transmissivity, selection of the relevant methods with the dataset and decision of the type of aquifers are important factors to keep in mind. To judge the type of aquifer system, first of all, drawdown is plotted with an arithmetic scale on the y-axis versus time plotted with a logarithmic scale on the x-axis for every wells were drawn and then fitted with a straight line. Afterwards, the behavior of the drawdowns points around the straight line are analyzed. The method suggested by Boonstra and Kselik (2001): (1) if the late-time drawdowns form a straight line under a slope, this generally indicates a confined or unconfined aquifer type (2) if the late-time drawdown form a horizontal straight line or a tendency towards stabilization, this generally indicates a leaky aquifer type (3) if the early-time drawdowns form a straight-line under a slope, this generally means that the aquifer is partially penetrated, are being applied in calibration. Moreover, the nature of lithologic succession and depth of static water level comparing with top boundary of the aquifer are taken into account. Generally, the Cooper-Jacob straight-line method is the best fit to the nature of dataset because well losses and partial-penetration will have a minimal effect on transmissivity values that are estimated using the Cooper-Jacob straight-line method by Halford and Kuniansky (2002). Transmissivity (T) is estimated from the pumping rate (Q) and the change in drawdown per log-cycle (Δs) from Equation 3.7.

$$T = \frac{2.3\,Q}{4\pi\Delta s} \qquad 3.7$$

Where

T = Transmissivity

Q = the discharge rate

Δs = change in drawdown per log-cycle

The result of hydraulic conductivity (K) & Transmissivity (T) values are mentioned in the Table 3.6 and the areal distribution map of results in Figure 3.7. Calculation details are shown in Appendix A2.

No.	well_name	Static level	elevation	K	T
1	Emirhac - 56395	69	1043.5	16	1400
2	Alibeyhüyügü - 56823	21	1020.4	3.8	470
3	Caldere - 51953	80	1018.7	2.4	240
4	Akincilar - 52967	39.7	968.7	120	7500
5	Besaglil - 51308	70	1038.9	67	3000
6	Katranci2 (Ipekler) - 5193	37	1049.8	16	1400
7	Topraklik - 53282	17	971.3	21	2700
8	Akorenkisla - 47890	40	1012.6	18	1400
9	Tasagil - 54890	9	1003.8	19	3800
10	Besci - 57232	100	1050	4.9	740
11	Ismil - 56237	25	996.9	9.1	510
12	Esmekaya - 52505	14.5	976.2	110	6000
13	Darihuyu u (Yapilcan) - 50516	2	929.6	5.1	320
14	Yenikent - 51391	9	920.2	19	1700
15	Incesu - 47722	23	963.2	2.5	190
16	Altinekin - 51379	33	929.6	4.6	540
17	Divanlar (Akbas) - 55525	23	995.3	11	770

Table 3.6. Hydraulic conductivity range from 17 pumping tests

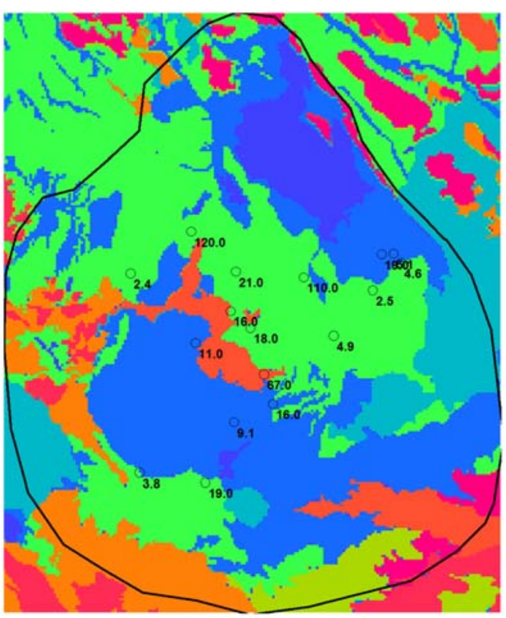

Figure 3.7. Distribution map of hydraulic conductivity (K) from pumping test

3.5.3. Result & discussion

The fact, that pumping tests were used to estimate aquifer properties at local scale, was elucidated by Sauter (1991) and his findings said that hydraulic conductivities (fissure & conduits) of the lower scale can serve as input for fissure hydraulic conductivity at the next higher scale. As Senturk (1969) described that well-developed karst nature is found in the Neogene aquifer, point measurement of pumping test at local scale range could not represent the regional flow scale.

3.6. Monthly measured hydraulic head

3.6.1. Available information

Dataset of the monthly measured groundwater level including 4 wells (1978-2009) and 45 wells (1998-2004) were received from DSI (State Hydraulic Works of Turkey).

3.6.2. Material & methods

In the monthly groundwater level dataset, there were some missing data in some months and unexpected abrupt head changed by several meter up or down during a short period may reflect measurement errors(Figure 3.8(a))to fill reasonably the gaps to remove unbelievable data and to analyse the fluctuation of groundwater nature and to correlate the relationship of the groundwater level changes and its neighbourhood, statistically analysis with the R application software was used.
For example Agabeyli well data comprises some missing data in some months and one pointed drop in 2003_2004. Such an big change of water level data will be negative effect and give some error ranges in calibration process. Akima spline interpolation method is chosen for all data set to fill gaps. (Figure 3.8(b))

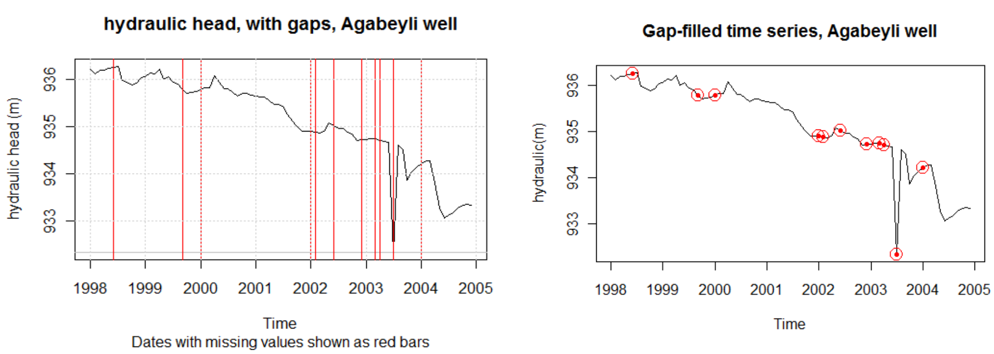

Figure 3.8. (a) abrupt drop of hydraulic head (b) gap filling with Akima spline interpolation

3.6.3. Result & discussion

3 wells of 8 years time serires and one well of 39 years time series were selected to illustrate the nature of groundwater in different zones according to head decline in Figure 3.9.
From box plot representation of 4 representative wells, the amplitude of Fethiye, Yorukcamilli wells vary about 1m until 2000 while Batum shows about 2m.The abrupt drop of groundwater starting from 2001 and then groundwater table rose back slowly in the late 3 years. During that same period, Agabeyli reflects groundwater drop continuously about 0.5m from 1998 to about 2m to 2004. In the 39 years long series analysis, Batum shows a small amplitude and variation of groundwater depth about 1-5m range during 1978-1993. After 1990, the increasing fluctuation dramatically occurred until 2009.

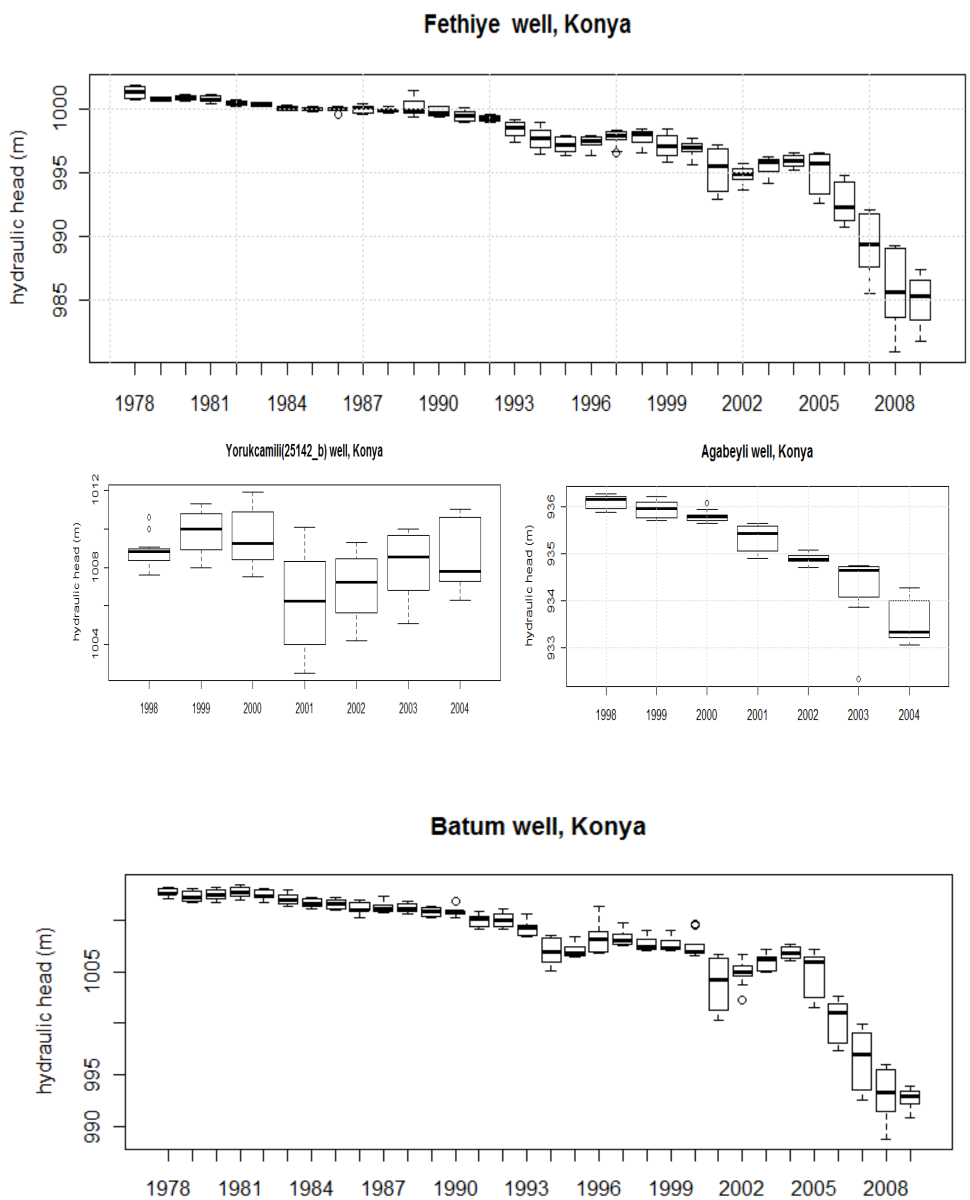

Figure3.9. The box plots show mean groundwater flow system and fluctuation of groundwater

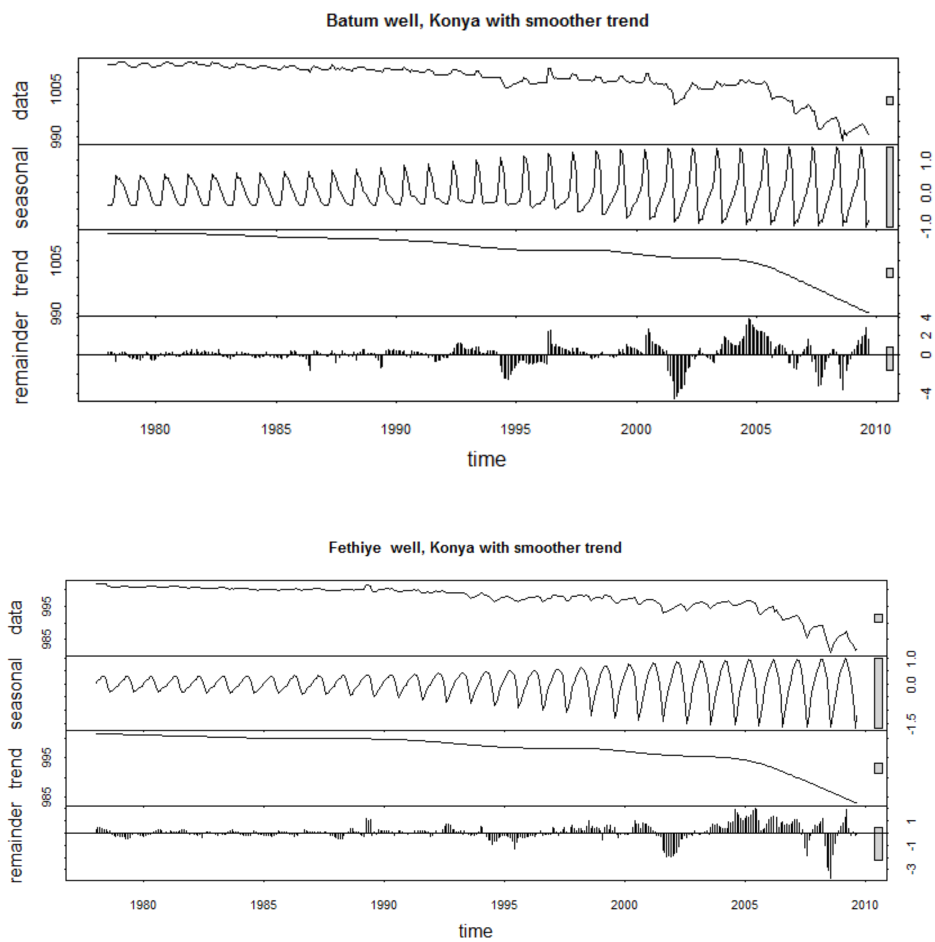

Figure3.10. Seasonal variation of hydraulic head

By analyzing with decomposition method in the 39years time series as “seasonal”, “trend” and “remainder”. Seasonally analysis is the best fit because groundwater table could not change in short time in nature. As shown in Figure 3.10, Fethiye well shows 2 times of head decline after 1996 while Batum well reflects in the same manner could easily be seen in long term series. Seasonal variation of groundwater table is in the range of -1 to +1m depth. Batum and Fethiye showed their trend range are about 25 m drop of groundwater table in the whole time-series.

4. RESEARCH METHODOLOGY

This chapter describes the development of the groundwater flow model. The conceptual set-up and the numerical model design of the Konya closed basin are discussed.

4.1. Defining conceptual model for KCB

The following steps are carried out in setting up a conceptual model.

- Model boundary definition
- Aquifer thickness definition
- Preliminary groundwater balance calculation
- Definition of flow directions and flow rate

4.1.1. Model boundary definition

Regional groundwater divides are considered as model boundaries(Figure 2.5). Although two major faults pass though the modeled area (Figure 2.4), those faults do not govern the regional groundwater flow system as shown in the cross-sections of the conceptual hydrogeological flow system (Figure 2.5) by Bayari, Ozyurt et al (2009).

4.1.2. Aquifer thickness definition

(a) Available information

The distribution of (28) bores map and (4) cross-sections pass through the study area are available. The Neogene aquifer is composed of two parts: Pliocene sands and conglomerates in the upper part and Miocene limestone with a basal conglomerate, alternated with marl in some places in its lower part. Alluvial deposit that represent aquitard system by Bayari, Ozyurt et al (2009) covers the southern Konya and northern Tuz lake sub-basins According to all cross-sections information supported by DSI (State Hydraulic Works of Turkey), alluvium deposits and Pliocene sediments are together defined as one unit and separate Miocene unit as a major aquifer system in cross-sections.(Figure 4.1**)** Therefore, two hydrostratigraphic units are represented as two model layers for the groundwater modelling, as described in the following subsections.

(b) Material & methods

(28) bore logs from cross-sections and extra-points from cross-sections of hydrogeological maps are used to transform into contour in ILWIS. The Dem surface was the assumed as a top of upper layer. The contact between the two hydrostratigraphic units were taken as a bottom boundary of upper layer that follows according to the elevation from the cross-sections. The bottom elevation of the Miocene unit represents as a base of lower layer. Contours were created based on points related to bottom elevation of each layers and interpolated into basements respectively. (Figure 4.2)

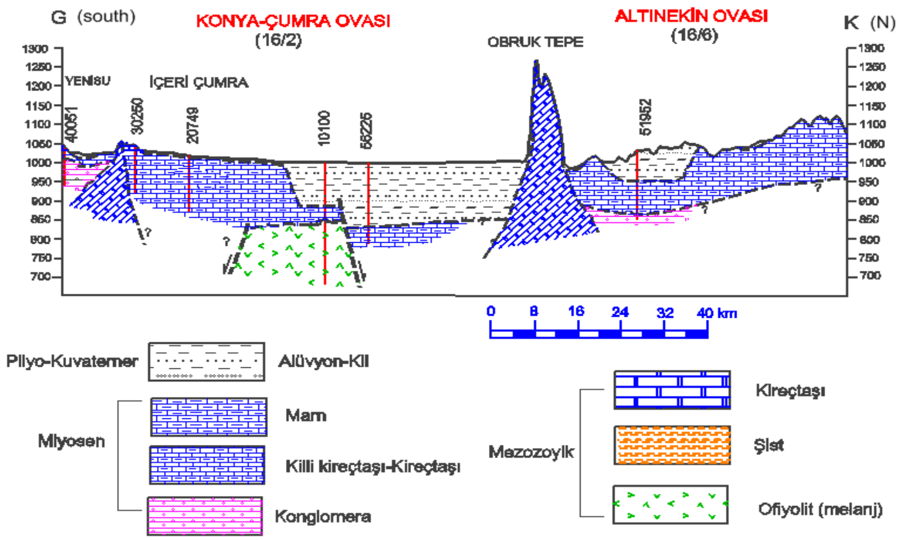
G (south)
KONYA-ÇUMRA OVASI
(16/2)
OBRUK TEPE
ALTINEKİN OVASI
(16/6)
K (N)
YENİSU
İÇERİ ÇUMRA
40051
30250
20749
10100
56226
51952
0 8 16 24 32 40 km
Pliyo-Kuvaterner
Alüvyon-Kil
Miyosen
Marn
Killi kireçtaşı-Kireçtaşı
Konglomera
Mezozoyik
Kireçtaşı
Şist
Ofiyolit (melanj)

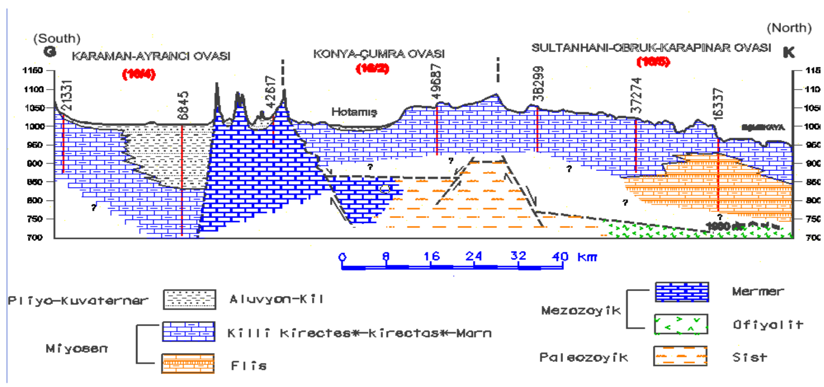
(South)
G
KARAMAN-AYRANCI OVASI
KONYA-ÇUMRA OVASI
SULTANHANI-OBRUK-KARAPINAR OVASI
(North)
K
21331
6845
42617
Hotamış
49687
38299
37274
16337
0 8 16 24 32 40 km
Pliyo-Kuvaterner
Aluvyon-Kil
Miyosen
Killi kirectas*-kirectas*-Marn
Flis
Mezozoyik
Mermer
Ofiyolit
Paleozoyik
Sist

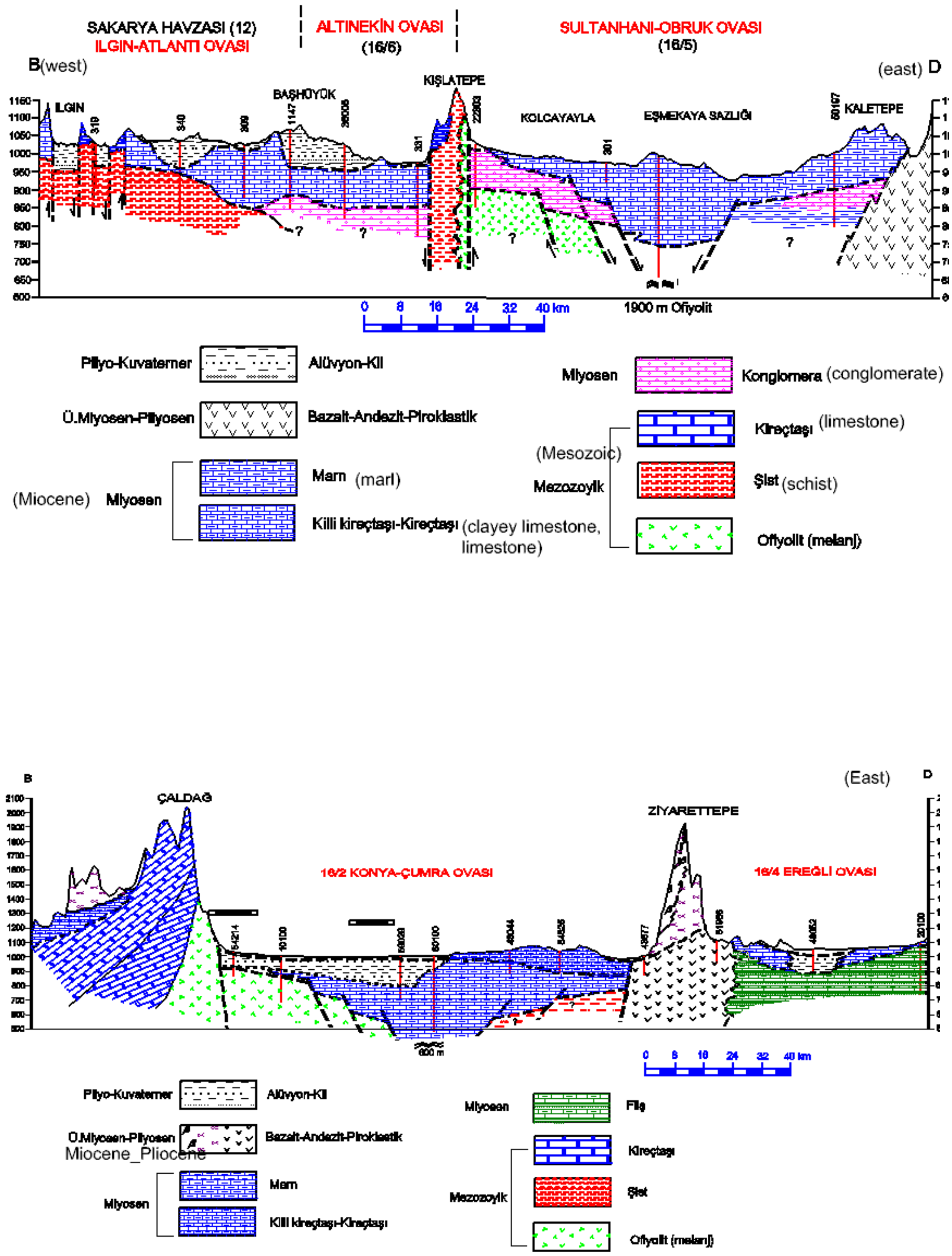

Figure 4.1 Geological cross-sections along N-S, and E-W direcions(source: unpublished data from DSI, Turkey)

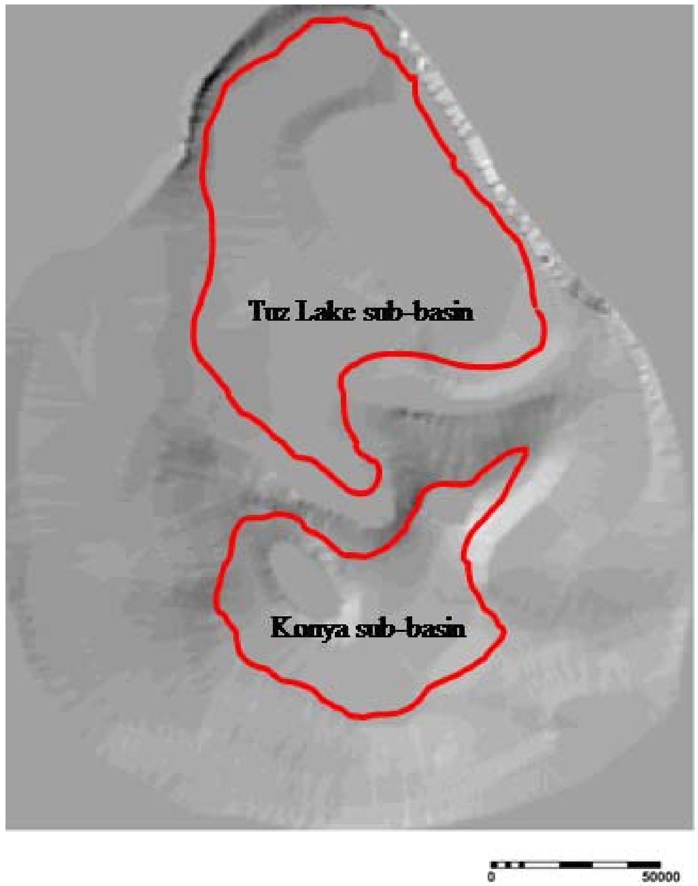

Figure 4.2 The bottom of the Neogene aquifer

(c) Result & discussion

Acording to cross-section interpretation, the deepest depth of the Neogene aquifer is 600m about in the southern Konya sub-basin. The depth about 150 m (estimated from the cross-section in Bayari, Ozyurt et al (2009) paper) reached to the aquifer base is found in Tuz Lake sub-basin. Generally, the thickness of the Neogene aquifer is about 200m in the study area. (Appendix A3) The geometry of the aquifer's thickness will help to estimate groundwater transmissivity and aquifer storage.

4.1.3. Preliminary groundwater balance calculation

(a) Available information

Groundwater system in the KCB discharges mostly into the Tuz Lake and the wetlands around it, from where the water evaporates. Furthermore, the water balance of the groundwater is determined by the precipitation, surface runoff, evapotranspiration and anthropogenic abstractions.

(b) Material & methods

The following components of groundwater balance will be calibrated in the model (Equation4.1).

$$\Delta S = Qgw\ in + R - (ETg + Qgw\ out) \pm A \qquad 4.1$$

Where,

ΔS = Change of aquifer storage

$Q_{gw\ in}$ = Groundwater inflow

$Q_{gw\ out}$ = groundwater outflow

R = actual recharge

ET_g = groundwater evapotranspiration

A = well abstraction/insertion

A basic assumption, that we can make on the basis of hydrogeological maps and cross sections is, that the study area is a closed basin and the flow of the groundwater discharges into the Tuz Lake. There is no outflow from the lake in the form of surface water, therefore, the groundwater inflow to the lake can be computed from the lake water balance equation by Nze (2010).

According to the available data (Chapter 3), direct precipitation over the Lake surface is 468.6 MCM/year, surface runoff to the lake is 291 MCM/year (Bayari, Ozyurt et al., (2009). Changes in lake water storage was calculated by previous MSc student (Nze, 2010); assuming 0.7 m as mean water depth in the lake and evapotranspiration from the lake, ETa as 1266.7 MCM/year, it results in a groundwater inflow of 506.42 MCM to the lake from the Neogene aquifer, as it is calculated by Equation 4.2.

$$Q_{gw\ in} = ETa - P - Q_{sw\ in} \pm \Delta S \qquad 4.2$$

Where,

ETa = evapotranspiration over the lake

P = precipitation over the lake

ΔS = changes in lake water storage

$Qsw\ in$ = surface runoff into the Lake

$Qgw\ in$ = groundwater flow into the Lake

For the other components in Equation 4.1, actual recharge should be lower than potential recharge of (2133 MCM/year) from the recharge map calculated in section 3.4, groundwater evapotranspiration is not considered for calibration in the model because the groundwater depths from the surface in the study are normally greater than 8 m in the in Konya-Curma plain, it varies 20-30 m in the Cihanbeyli and Aksaray plains, the deepest range is about 60-70 m at the Taurus mountain flank. Change of aquifer storage is only applicable for transient solution. Wetland evaporation (278.21 MCM/year) in Table 3.4 and abstraction at the irrigation areas (5.2 MCM/year) in Appendix A5 were considered as groundwater losses. Calculation results are shown in Table 4.1.

1		Influxes	Outfluxes	
	precipitation(MCM	inflow from Beysehir(MCM)	evapotranspiration(MCM)	balance(MCM)
	468.6	134	7791.5	-7188.9
2				
	precipitation	inflow from Beysehir	abstraction	
	468.6	134	1906	-1303.4

Table 4.1. Comparison between influx and outflux (year 2002)

(c) Result & discussion

All results are based on year 2002. According to the preliminary results budgeting, the low precipitation, high evapotranspiration rate and huge groundwater abstraction are threatening groundwater scarcity.

4.1.4. Definition of flow directions and flow rate

(a) Available information

According to the conceptual hydrogeologic model of the regional groundwater flow in Bayari, et al.(2009), there is a topography-driven groundwater flow from the Taurus Mountains (main recharge area) towards the Tuz Lake (main discharge area). The groundwater head distribution in KCB as described by Senturk (1969) is as follows: the general hydraulic head at the Taurus mountain flank is about 1,100m and it decreases to 920m around the Tuz Lake. A slight increase of hydraulic head is encountered in the middle plateau which represents an intermediate recharge zone. The result of the study based on the radio carbon age determination by Bayari, et al.(2009), the rate of the regional groundwater flow is (3m/year) due to the low hydraulic conductivity of the Quanternary deposit..

4.2. Defining Numerical model for KCB

Numerical groundwater model based on Darcy's law, which assumes laminar flow, was applied in the KCB. In reality, the basically porous Neogene deposits form a somewhat karstified aquifer system, with unknown amounts of secondary (fracture) or tertiary (conduit) flows , which may be problematic in this type of simulation. However, a porous medium flow model can be developed in karst aquifer, as long as its limitations are acceptable, as suggested by Scanlon, Mace et al (2002) .
The basic intention was develop a steady-state model for simulating the general flow conditions. In case of successful modelling, this can provide a starting point for further transient modelling in the future.

4.2.1. Software & type of model

The software Processing Modflow for Windows (PMWIN) and MODFLOW-96, Harbaugh and McDonald (1996) were selected to simulate the groundwater system of KCB. The MODFLOW software is a device to simulate groundwater flow by means of the Darcy's equation. To minimize the effects of the unknown preferential secondary and tertiary flow systems, a large grid size was selected.

4.2.2. Boundary conditions

The area (1725 km^2) of Tuz Lake cells are simulated as constant-head boundary. The regional water divides mentioned in Figure 2.5 are assigned as no flow boundaries. Impermeable bed rock of the model is also defined as a no-flow boundary. (Figure 4.3)

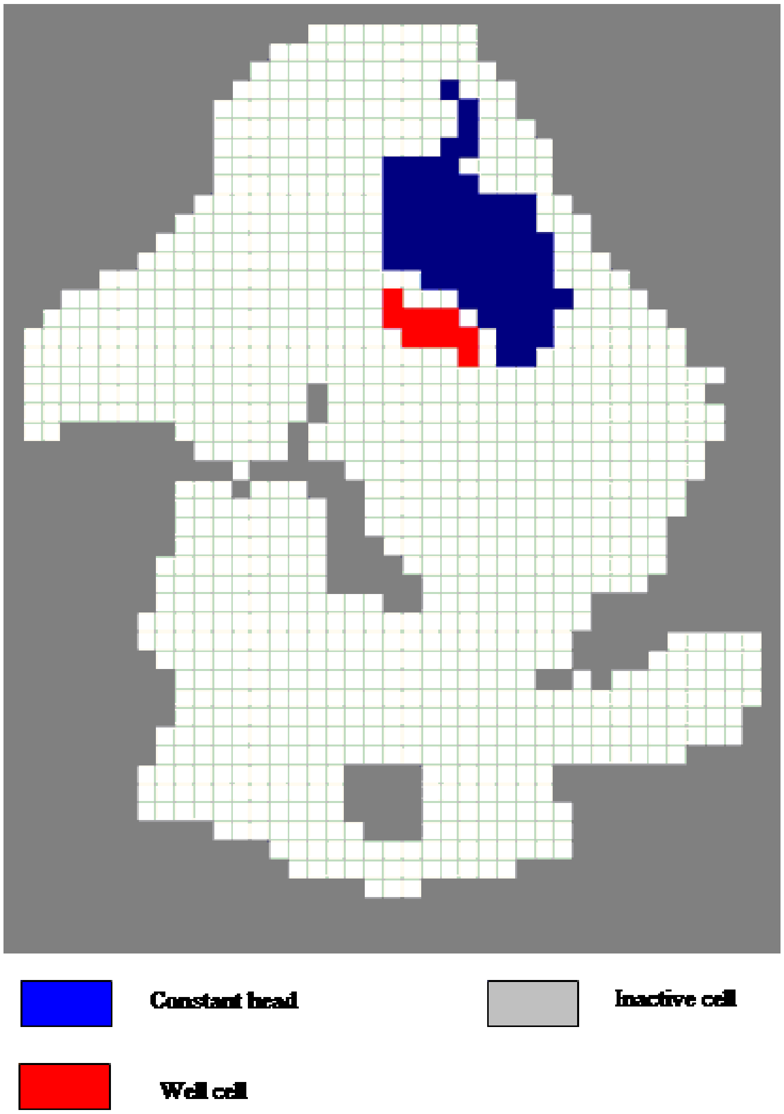

Figure 4.3. Boundary conditions of the model

4.2.3. Hydrostratigraphic units

A three-dimensional model was developed with two aquifer layers: the Pliocene aquifer as the upper, and the Miocene as the lower layer. In places where the Pliocene is missing, the Miocene aquifer was divided into two layers. Upper layer was designed as unconfined system, whilst the lower layer was constructed as a mixed aquifer system, which may vary spatially from unconfined to confined conditions.

4.2.4. Grid design

Coarse square grid size of 5km x 5km was selected due to the large extent of the study area. Although the model layers represent a karst carbonate aquifer in the KCB, which may have conduit flow and fissure flows, it is assumed that at the scale of the coarse grid cells it can be modelled as an equivalent porosity medium (EPM) by Anderson and Woessner(1992).

4.2.5. Input parameters

All input parameter units are in meters and calibration is on a daily basis.

(1) Recharge

A daily recharge spatially distributed map is obtained by the wet season recharge map calibrated in section 3.4.2 which was divided by 365 days. Total upper limit volume of daily average recharge map, 5.84 MCM/day is prepared for calibration. This is composed of the recharge for the low lying areas, which is 5.25 MCM/day, and the recharge as a mountain runoff, equivalent to 0.59 MCM/day. The mountain cells are represented as inactive cells. The mountain runoff recharge is distributed to each of the active cells in the low-lying areas closest to the mountain cells. This is like assigning the cell as injection well only that the method is done in the recharge package of MODFLOW instead of the well package.

(2) A set of hydraulic head

A set of hydraulic head read in 1966 hydrogelogic map are interpolated and converted into ASCII form to represent initial hydraulic head for calibration. For a steady state solution, a good set of starting heads makes the solution converge faster, although the effect of initial condition does not influence the solution..

(3) Sinks and sources

The wetland area around the Tuz Lake evaporates with the rate of 0.76 MCM/day on average. That area was considered as a sink to abstract water from the system and simulated as well cells. (Figure 4.3)

(4) observation wells

Total (16) hydraulic heads from 1966 hydrogeologic map in (Appendix A4) are read to serve as the observation wells. Those heads represents the aquifer is at pristine state and not influenced much by abstraction in agreement with the hydraulic head distribution at that time which shows a topography-driven groundwater flow from the southern mountain region towards the Tuz Lake.

5. CALIBRATION AND PREDICTION

This chapter presents the calibration of the groundwater flow model, which was followed by running the model to simulate abstraction scenarios.

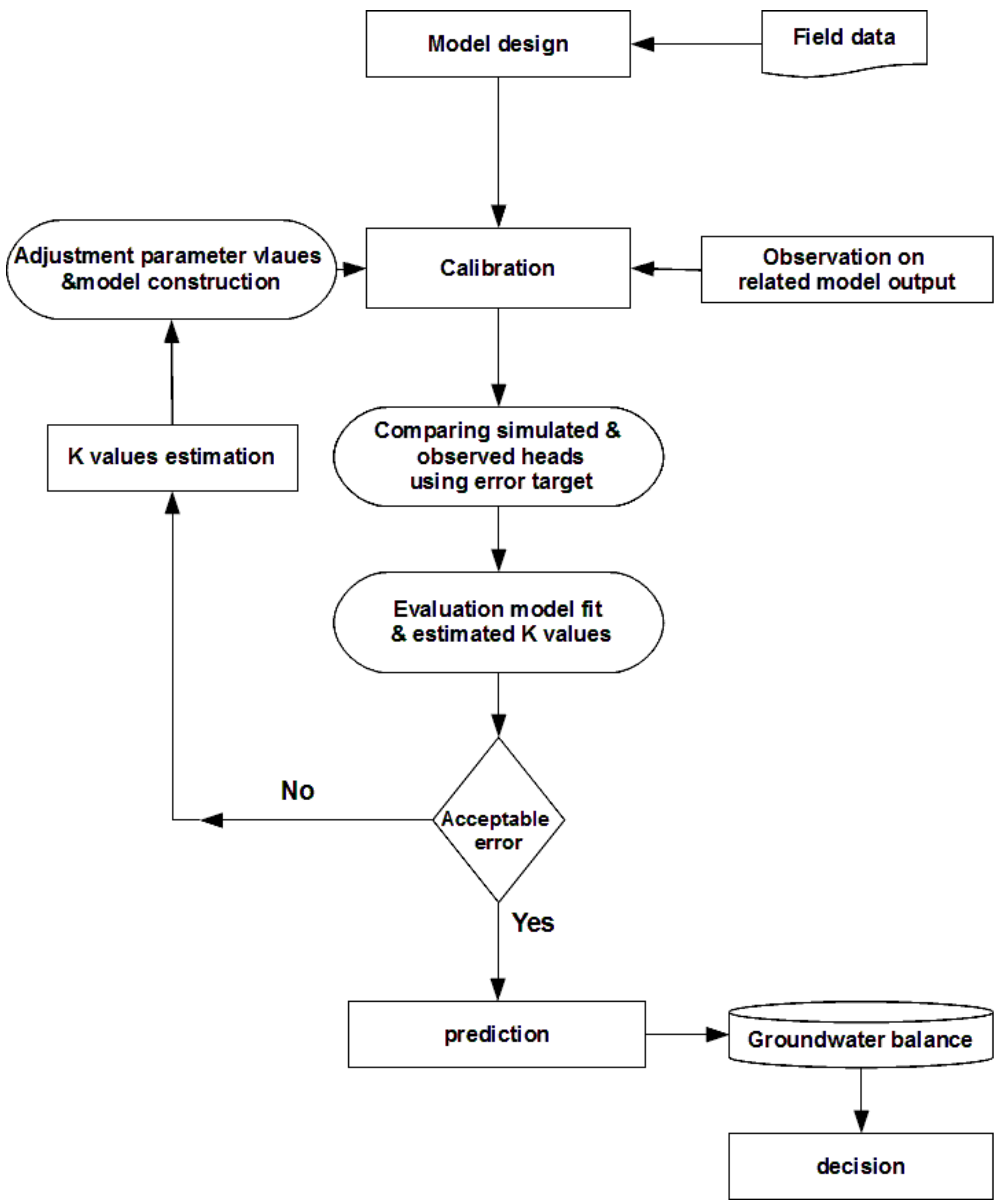

Figure 5.1. A flow chart of model calibration steps

5.1. Calibration process

(a) Steady state calibration

Steady state calibration is furnished by finding a set of hydraulic conductivity (K) parameter based on the concept of Equation 5.1.

$$K_1D_1I_1=K_2D_2I_2=K_3D_3I_3\ldots\ldots \qquad 5.1$$

Where,

K =hydraulic conductivity

D =thickness

I =hydraulic gradient

The thickness map is the only static input parameter. The hydraulic gradient changes in response to the adjustments in hydraulic conductivity, and this produces the changes in head. At the end of each run, MODFLOW reports the water balance output which includes the report for recharge and discharge values.

The controlling factors and target values in the model are the following: constant head in the lake, aquifer discharge to the lake of 0.6 MCM/day according to Bayari, Ozyurt et al (2009) and get a water balance (input =output). The recharge is adjusted while maintaining the constant head in the lake and aquifer discharge to the lake close to the target value. The target value of 0.6 MCM/day was not reached, however, the aquifer discharge to the lake of 1.44 MCM/day represents a more balanced groundwater system. The computed recharge to the aquifer is then 2.2 MCM/day, where 1.44 MCM/day is aquifer discharge into the lake. Subsequent model calibration involved the adjustments of hydraulic conductivity starting with hydraulic conductivity values from pumping tests to match the simulated heads and flows with the calibration target which are the pristine head values (of 1966). Depending on the differences between the measured hydraulic heads and the calibrated heads, the errors were measured with mean and standard deviation after every simulation with different hydraulic conductivity. The results of error discrepancy, groundwater budget, groundwater flow system and hydraulic conductivity matrix, in the system are shown in Figures 5.2, 5.3, 5.4, 5.5, 5.6 and Tables 5.1, 5.2.

Initial attempts to calibrate hydraulic conductivity with automated inverse method described by Bridget R. Scanlon, Robert E. Mace et al (2002) was not successful in producing the defined zones of varying hydraulic conductivity. Therefore, manual trial-and-error calibration was applied to find the optimum model parameters, which represent the measured hydraulic heads from 1966 hydrogeologic map to get the pristine state.

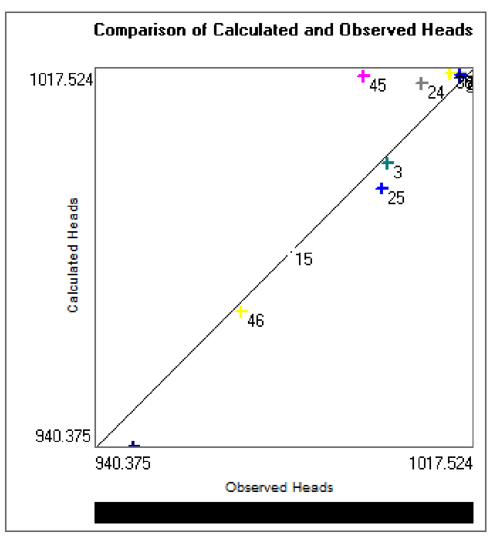

Figure 5.2 Scatter diagram of 16 wells' hydraulic head distribution in the correlation line

well no	elevation((m) DEM	measured head (m)	computed head (m)	hm-hs(m)
1	957.3	948	941.375	-6.625
3	1007.6	1000	998.3834	-1.6166
7	1012.7	1015	1016.695	1.695
9	1020.4	1015	1016.321	1.321
12	1019	1015	1015.635	0.635
15	985	980	980.5432	0.5432
17	1032.2	1015	1016.325	1.325
22	1093.6	1020	1022.46	2.46
24	1004	1007	1012.541	5.541
25	1008	999	993.2124	-5.7876
30	1034.9	1013	1015.384	2.384
33	1015.7	1015	1015.602	0.602
41	1011.6	1015	1012.474	-2.526
45	994	995	1006	11
46	902.2	970	967.0598	-2.9402
Timras	1038.4	1020	1021.9	1.9
mean				0.534053333
standard deviation				4.190218072

Table 5.1. Error calculation between measured and calibrated heads

```
PMWBLF (SUBREGIONAL WATER BUDGET) RUN RECORD
FLOWS ARE CONSIDERED "IN" IF THEY ARE ENTERING A SUBREGION
THE UNIT OF THE FLOWS IS [L^3/T]

TIME STEP   1 OF STRESS PERIOD   1

=========================================================
WATER BUDGET OF THE WHOLE MODEL DOMAIN:
=========================================================

FLOW TERM            IN               OUT              IN-OUT
STORAGE              0.0000000E+00    0.0000000E+00    0.0000000E+00
CONSTANT HEAD        0.0000000E+00    1.4414125E+06    -1.4414125E+06
WELLS                0.0000000E+00    7.6000000E+05    -7.6000000E+05
DRAINS               0.0000000E+00    0.0000000E+00    0.0000000E+00
RECHARGE             2.2014125E+06    0.0000000E+00    2.2014125E+06
ET                   0.0000000E+00    0.0000000E+00    0.0000000E+00
RIVER LEAKAGE        0.0000000E+00    0.0000000E+00    0.0000000E+00
HEAD DEP BOUNDS      0.0000000E+00    0.0000000E+00    0.0000000E+00
STREAM LEAKAGE       0.0000000E+00    0.0000000E+00    0.0000000E+00
INTERBED STORAGE     0.0000000E+00    0.0000000E+00    0.0000000E+00
MULTI-AQIFR WELL     0.0000000E+00    0.0000000E+00    0.0000000E+00
---------------------------------------------------------------
      SUM 2.2014125E+06  2.2014125E+06  0.0000000E+00
DISCREPANCY [%]  0.00
```

Table 5.2. Water balance in the model system at steady state simulation.

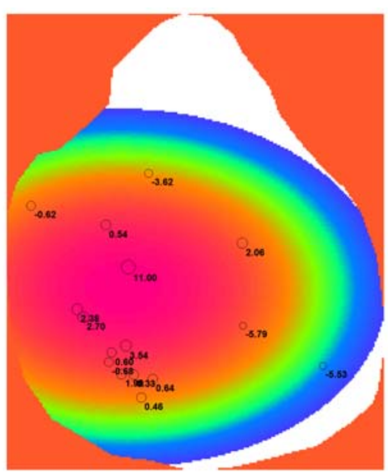

Figure 5.3. Error distribution map (unit in meter)

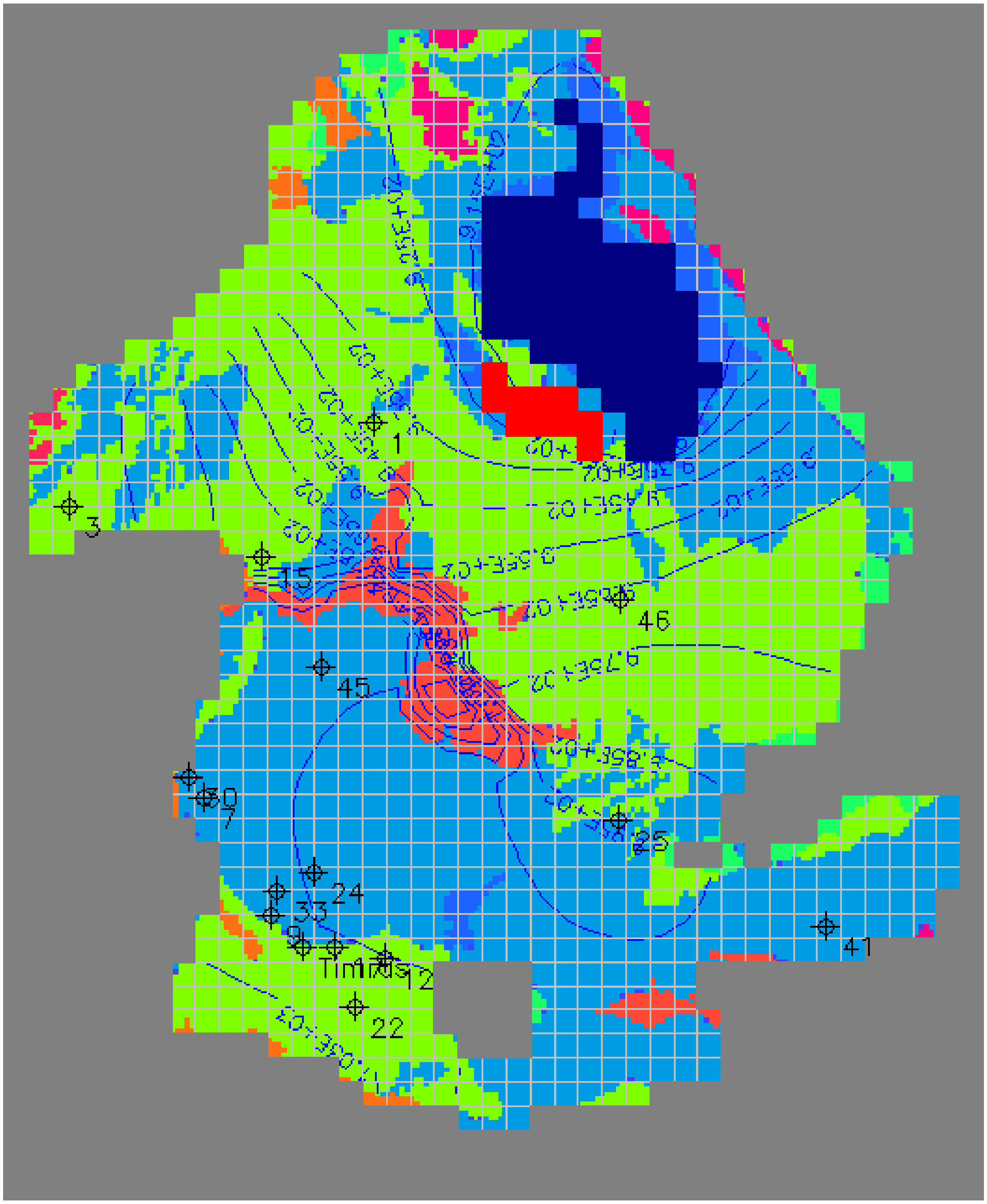

Figure 5.3. Simulated groundwater flow system in KCB

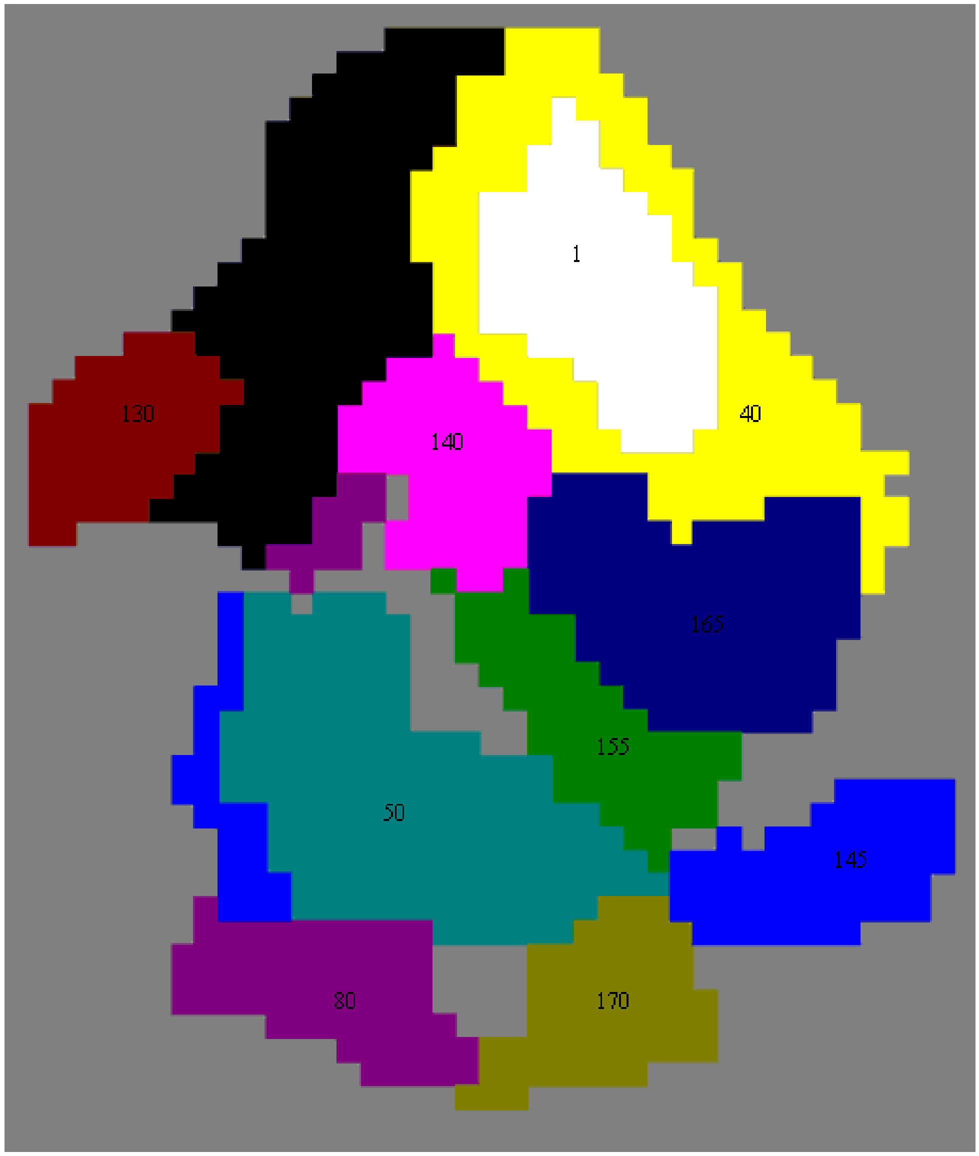

Figure 5.4. Spatial hydraulic conductivity map of upper layer after steady state simulation

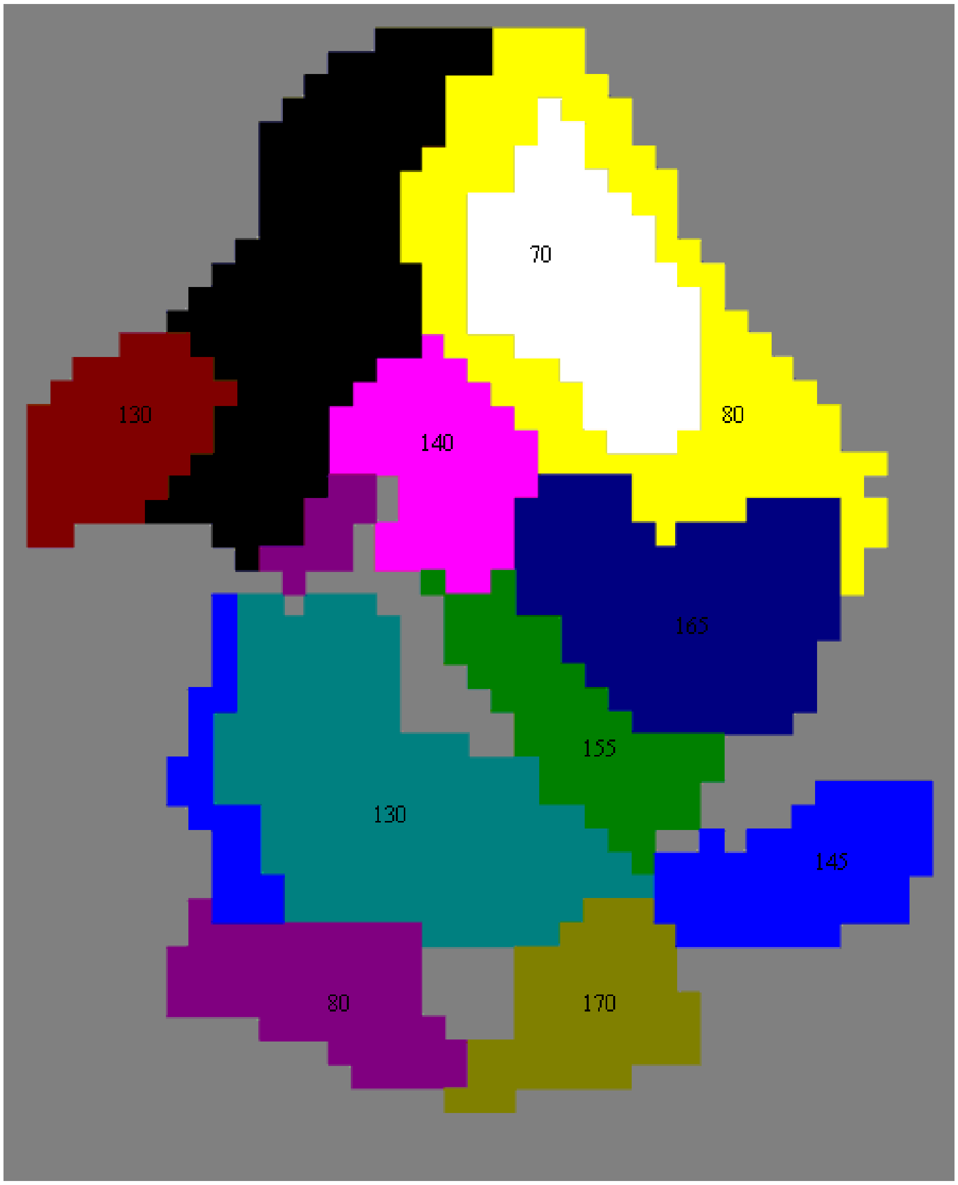

Figure 5.5. Spatial hydraulic conductivity map of lower layer after steady state simulation

(b) Result & discussion

First of all, the calibrated hydraulic conductivity (K) values are different from the measured values. The point estimates of the hydraulic conductivity could not represent the bulk hydraulic conductivity because of scaling effects, as described by, e.g., Bridget R. Scanlon, Robert E. Mace et al. (2002). the simulated hydraulic head is about 1030 m around the Taurus mountain flank, and gradually decreases to 925m around the Tuz lake. Figure (5.4).

In the region of the location (4751000, 423000), with the groundwater is passing through the middle mountain range between the two sub basin with a head of 983 m. The southern, Konya basin has hydraulic head variations between 1015-1000 m. In the Tuz Lake basin, the general hydraulic head changes from 980 m to about 925 m from the south towards the Tuz lake. Detailed analysis of the scattered plot that represents the differences between measured hydraulic heads and the calibrated heads shows a high discrepancy at well no. 45. The hydraulic head of this well was found to be higher than the

ground surface, which indicate the area can be considered as artesian area. In the model, the hydraulic head in the Timras sinkhole showed 1020 m. By comparing this to a present time hydraulic head of 1006 m (average head in 2002), it can be concluded that the groundwater surface became lower by 16m during 36 years.
A mean error of 0.5 m and a standard deviation of 4 m were obtained at regional scale, which were considered as acceptable. Mean error reflects there is an average 0.5 m higher in calibrated heads mostly than the heads at the prinstine state.
Concerning the groundwater budget results, model was calibrated to 2.2 MCM/day as a total recharge component. From this total, 0.76 MCM/day is evaporated by the wetland area and the rest (1.44 MCM/day) terminates at the constant head of the Tuz Lake is shown in Figure 5.7.

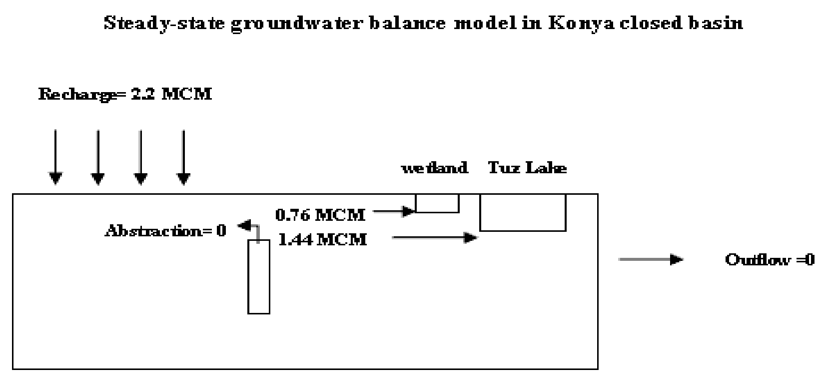

Figure 5.6 Schematic diagram of steady state modelling

5.2. Prediction

(a) Prediction process
Two irrigation areas: Konya-Curma (16/2) and Sultanhani-Obruk-Karapina (16/5) were encountered according to the information from DSI(State Water Authority) in Appendix A5.
Total abstraction amount in the year 2010 concerning the sub-basins16/2 and 16/5 is 1900 MCM. This is in agreement with the magnitude of the information by Bayari, Ozyurt et al (2009); an annual groundwater abstraction rate of 2600 MCM/year. On the other hand, the amount of actual evapotranspiration found in section 3.3 is significantly higher for the irrigation areas (7791.50 MCM/year).
When the model was run in the transient mode with the abstraction scenarios of the lowest amount (1900 MCM/year = 5.2 MCM/day), the model almost dried out within a year, even when a high specific yield of 0.25 was applied for both layers although a specific yield of 0.15 is generally suggested for karst aquifers, as described by Bolster CH, Genereux DP et al. (2001). The paper indicates that for a highly transmissive limestone aquifer at a large spatial scale, estimation of storage parameters from the pumping tests would be impractical and not representative. Therefore, results of pumping tests from other reports were discarded from the further work.

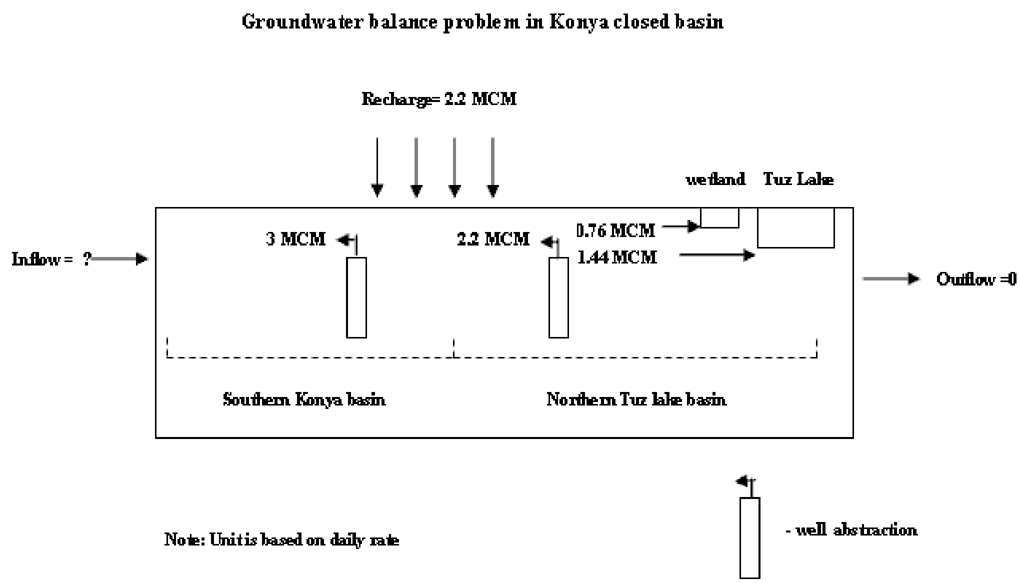

Figure 5.7. A schematic diagram shows groundwater balance problem in Konya

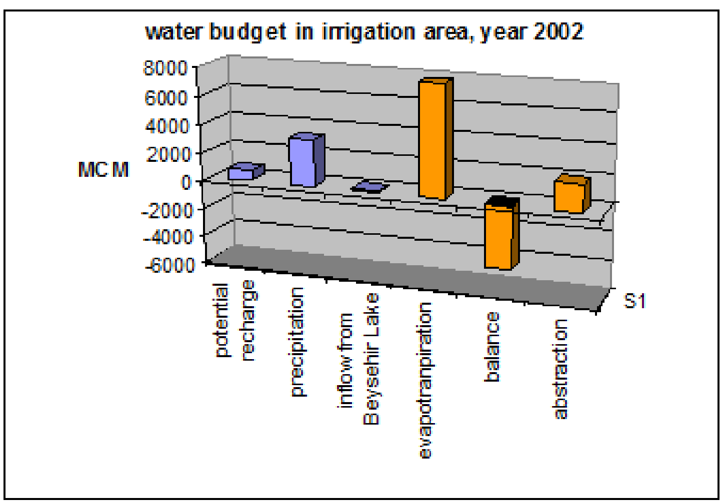

Figure 5.8. The diagram represents surface water balance problem

(b) Result & discussion

The low recharge value of 2.2 MCM/day found by the model calibration could not recover the huge abstraction rate of 5.2 MCM/day. (Figure 5.8) The model was constructed with the target to balance the total discharge amount from the Neogene aquifer towards the Lake according to the information that the groundwater flow passing through the Neogene aquifer terminates to the lake with an average amount of 233 MCM/year discharge as described by Bayari, Ozyurt et al. (2009). However, when the huge abstraction amount in the irrigation areas are considered, the water budget by the model results in high discrepancy between the influxes and evapotranspiration relatively shown in Figure 5.9.
The actual evapotranspiration 7791.5 MCM/year estimated from satellite images by Gokmen (2009) is much higher than the abstraction amount of 2600 MCM/year given by the water authority. The difference cannot be covered by both of the precipitation 2133 MCM/year and the surface inflow from the Beyehir Lake of 134 MCM/year.

Generally speaking, if such a huge amount of evapotranspiration does not come from precipitation or any other surface inflow components, there is only the groundwater resource to compensate the evapotranspiration component, i.e. there might be more pumping going on then what the water authorities account for. This extra volume has to be provided by the groundwater flow. However, when aquifer storage capacity was raised for this purpose, the volume of discharge to the Tuz Lake became larger because the model responses the volume discharge to the constant head became larger. Therefore, there have to be other groundwater inflow components to the aquifer system together with higher hydraulic conductivity than the present calibrated one. Since this inflow existed in the 'pristine' conditions too, so this extra water had to be evaporated before it reached the Tuz Lake (there is no evidence available that the Tuz lake was considerably bigger before the intensification of pumping, so this extra water was not evaporated from there).

However, in the Konya sub-basin, there were in the past some wetlands and artesian zones which were near to the flanks of the middle mountain range. This is in agreement with the information of hydrogeology map (1966). Such a hydrogeologic regime mostly disappeared in the present time because of high abstraction rates in that region. This means that subsurface inflow from the mountain ranges can mix with the Neogene aquifer system to make Neogene aquifer flows higher. Similarly, the inflow from the mountain ranges can occur also in the Tuz Lake sub-basin. As a result, some parts of shallow local flow system in Konya sub-basin used to discharge in to the local wetlands in the pristine state and could not reach to the Tuz Lake, while the regional groundwater flow system through the Neogene aquifer flows to the Tuz Lake. In summary, the Tuz lake is not the only terminate for all of the groundwater flow systems from the Neogene aquifer.

A schematic diagram was created to reflect how the groundwater flows in Neogene aquifer system in Figure 5.10 .The model area represents only the Neogene aquifer, and the two major irrigation zones in Konya and Tuz Lake sub-basins.

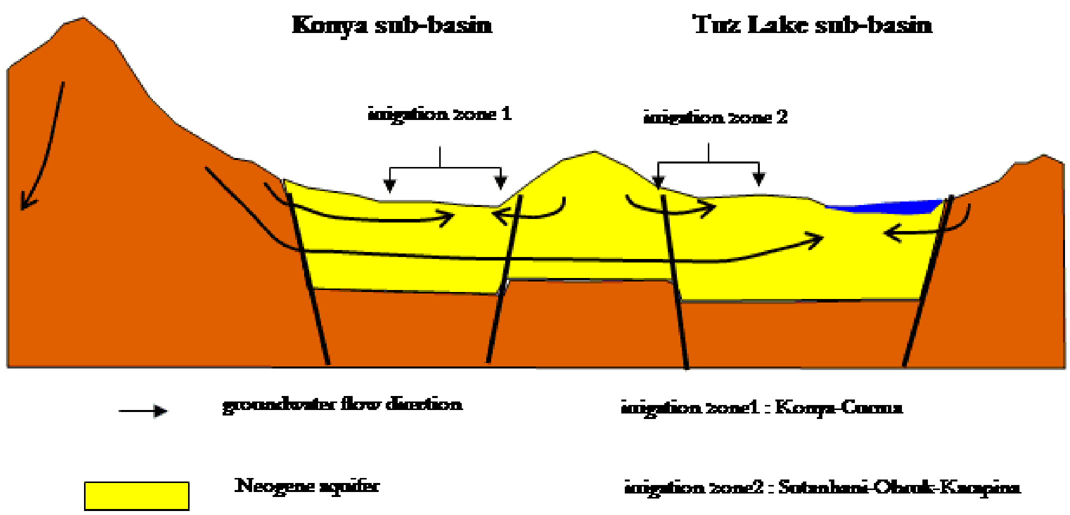

Figure 5.9 The schematic diagram represents the groundwater flow system in KCB

6. CONCLUSION AND RECOMMENDATIONS

MODFLOW-96 (Harbaugh and McDonald (1996) was used to quantify the groundwater fluxes in the Konya closed basin in a spatially distributed manner. MODFLOW-96, which is a porous medium based numerical groundwater flow model,was applied in a karst aquifer in this case. 5 x5 km cell size, was found to be large enough to approximate equivalent porous medium in this karst systems.

6.1. Conclusion

The wet season orographic rainfall map was created by using linear function between the elevation of the meteorology stations and total monthly rainfall for the whole wet season. The actual monthly rainfall maps were produced by adding the monthly averaged orographic rainfall maps together with the differences between averaged monthly orograpic rainfall and monthly measured rainfall. When the value of evapotranspiration is larger than precipitation at a cell, zero recharge was applied for the cell. Finally recharge assessment was carried out by subtracting the evapotranspiration from precipitation. Considering the mountain front system in KCB, a small amount of 10% of direct precipitation as mountain runoff is expected along the foothills and this was added into recharge map to avoid underestimation of recharge value. The result of potential recharge 5.84 MCM/day is an upper limit of the probable recharge to the groundwater table. The result is still composed together with soil water storage. To obtain actual recharge map, soil water storage capacity should be calculated.

Geometry of the Neogene aquifer system was constructed in two layers: upper layer is unconfined type and lower layer is unconfined/confined of mixed system. The thicknesses of both layers were defined by interpolation.

Steady-state calibration of the hydraulic conductivities was carried out to obtain spatially distributed average hydraulic heads. Measured hydraulic heads from hydrogeologic map (1966) were used to evaluate the steady state model calibration because the aquifer was almost at pristine state in the late 1960, as described by Bayari, Ozyurt et al. (2009). Initial attempt to calibrate hydraulic conductivity with automated inverse method could not produce the defined zones of varying hydraulic conductivity described by Scanlon, Mace et al (2002) . Therefore, manual trial and error calibration was applied to obtain the optimum model parameters. The set of hydraulic heads at pristine state were compared to the corresponding calibrated heads in every simulation during the calibration process, to reach the calibration target. An acceptable mean error of 0.5 m and a standard deviation of 4 m were obtained at regional scale. According to the results, the hydraulic conductivity varies around 110-170 m/day in the lower stratigraphic unit and same ranges were given in upper layers except the confined system. While the hydraulic conductivity for high alluvial thickness in Koya-Cumra area was given 50 m/day, it was assigned as 1m/day for the alluvium under the Tuz Lake as adopted directly from Bayari (2009). It can be noted that the spatial distribution and the actual values of the calibrated hydraulic conductivities are quite different from the measured values obtained by pumping tests. Therefore, it can be concluded that such point estimates of hydraulic conductivity cannot represent the bulk hydraulic conductivity at regional scale because of scaling effects as described by Bridget R. Scanlon, Robert E. Mace et al. (2002).

By detailed analysis of the discrepancies between the measured heads and the simulated heads, an artesian area was observed since the hydraulic head was higher than the ground surface during calibration. By comparing the present time hydraulic head of Timras Sinkhole (Obruk) which is 1006 m that represents average head in 2002, the hydraulic head became 16 m lower during last 36 years.

According to the groundwater budget results provided by numerical model, a total recharge of 2.2 MCM/day was found as the upper limit in steady state simulation.

A sensitivity analysis and further evaluation of hydraulic head in the calibrated model are recommended to quantify the uncertainty of the calibrated model parameters and to improve the estimation of aquifer parameters, stresses and boundary conditions.

The model failed in quasi-transient mode due to unbalanced huge abstraction rate of 5.2 MCM/day in the Neogene aquifer. Low recharge of 2.2 MCM/day that is balanced by model calibration, could not recover the huge abstraction rate of 5.2 MCM/day. The model was constructed with the target to balance the total discharge amount from the Neogene aquifer towards the lake according to the discharge of 0.6MCM/day given by Bayari, Ozyurt et al. (2009). In this regard, it was assumed in the model setting that all of the groundwater flow in the Neogene aquifer terminates in the Tuz Lake.
However, it was found that Neogene aquifer was not in balance due to the high evapotranspiration outflux 7791.5 MCM/year, low precipitation influx with an upper limit of 2133 MCM/year,. Therefore, the assumption that groundwater flow through Neogene aquifer terminates only at the Tuz Lake is not correct and there has to be other groundwater inflow/outflow components to/from the aquifer system.
If the result of head changes was possible to fit in quasi-transient mode to predict future, the head changes could represent hydrogeological environments such as lakes, wetlands and springs etc. related to the Neogene aquifer and environmental impacts could be estimated. If the head decline rate could be determined, the available groundwater reserve could be calculated and it could be estimated how long the aquifer could yield water applying the same rate of abstraction as now. Then, further calibrating the aquifer storage capacity, the ecological groundwater demand of KCB could be estimated. Therefore, the numerical groundwater modelling was found to be an important tool to estimate the spatio-temporal distribution of groundwater fluxes.

6.2. Follow up research

Further studies should focus on improving the existing model in several ways such as by removing the assumption that all of the groundwater flow components from the Neogene aquifer discharge to the Tuz Lake because the current model suggests that additional outflows existed even in the pristine conditions.
Future studies should consider adding an inflow component from the mountains to the aquifer besides the inflow component from the mountain surface runoff because most of the mountain ranges in KCB are in karstic nature of pleozoic-mesozoic aged marine carbonate origin in the southern part of the model, and this system was proved by the modelling to be linked to the Neogene aquifer. In the east, the volcanic terrains surround the KCB basin and the inflow from those mountains would be quite different in comparison with the southern terrain. Therefore, the aquifer properties and the boundary conditions need further adjustments for a more accurate definition of the model. Parameterization of the distributed model depends on accurate information on hydraulic head and thus future studies should improve the reliability of the head data by accurately locating wells and measuring surface elevation because such kind of data set is also reliable for evaluating the calibration. A greater number and a wider distribution of head measurements would improve the parameterization of the distributed model.
Combining manual trial-and-error methods and automated inverse procedure is recommended to generate an optimized model with better distribution of hydraulic conductivities.

LIST OF REFERENCES

Bayari, C. S., N. N. Ozyurt, et al. (2009). "Radiocarbon age distribution of groundwater in the Konya Closed Basin, central Anatolia, Turkey." Hydrogeology Journal **17**(2): 347-365.

Bayari, C. S., E. Pekkan, et al. (2009). "Obruks, as giant collapse dolines caused by hypogenic karstification in central Anatolia, Turkey: analysis of likely formation processes." Hydrogeology Journal **17**(2): 327-345.

Bolster CH, Genereux DP, et al. (2001). "Determination of specific yield for the Biscayne Aquifer with a canal-drawdown test." Hydrogeology Journal **39(5):**: 768-777.

Boonstra, J. and R. A. L. Kselik (2001). "SATEM 2002: Software for Aquifer Test Evaluation." Retrieved 20.2.11, from http://www2.alterra.wur.nl/Internet/webdocs/ilri-publicaties/publicaties/Pub57/pub57-h8.pdf.

Brutsaert, W. (2005). Hydrology. New York, the United State of America, Cambridge University Press.

Fontugne, M., C. Kuzucuoglu, et al (1999). From Pleniglacial to Holocene: a C-14 chronostratigraphy of environmental changes in the Konya Plain, Turkey, Pergamon-Elsevier Science Ltd.

Gökmen, M. (2009). Earth observation for Quantifying ecohydrological Fluxes and Inter-Relations. Unpublished PhD Research Proposal, International Institute for Geo-information Science and Earth Observation.

Halford, K. J. and E. L. Kuniansky (2002). Documentation of Spreadsheets for the Analysis of Aquifer-Test and Slug-Test Data. Open-File Report 02-197. Carson City, Nevada, U.S. Geological Survey.

Harbaugh, A. W. and M. G. McDonald (1996). User's documentation for MODFLOW-96, an update to the U.S. Geological Survey modular finite-difference ground-water flow model. , U.S. Geological Survey**:** Open-File Report 96-485: 456.

Lubczynski, M. W. (2006). Groundwater fluxes in arid and semi - arid environments. Groundwater and ecosystems : NATO advanced research workshop on groundwater and ecosystems, Canakkale, Turkey, Springer: 225-236.

Meester, T. (1970). The soils of the Great Konya Basin. Agricultural Research Reports. Wageningen, Agricultural University, Department of Tropical Soil Science**:** 290.

Nze, O. K. E. (2010). Assessing the groundwater dynamics in a semi - arid region. MSc Thesis. Enschede, ITC**:** 54.

Sauter, M. (1991). "Assessment of hydraulic conductivity in a karst aquifer at local and regional scale ". from http://info.ngwa.org/GWOL/pdf/920156209.pdf.

Scanlon, B. R., R. E. Mace, et al. (2002). "Can we Simulate Regional Groundwater Flow in a Karst System Using Equivalent Porous Media Models? Case Study Barton Springs Edwards Aquifer, USA." Journal of Hydrology **276**(1-4): 137-158.

Senturk, F. (1969). Isotope techniques applied to groundwater movement in the Konya Closed Basin. Ankara, State Hydraulic Works(DSI), Groundwater and Geotechnical Services Division.

Su, Z. (2002). "The Surface Energy Balance System (SEBS) for estimation of turbulent heat fluxes." Hydrology and Earth System Sciences 6(1): 85-99.

Tempfli, K., N. Kerle, et al., Eds. (2009). Principles of Remote Sensing. ITC Educational Textbook series. Enschede, The Netherlands, The International Institute for Geo-Information Science and Earth Observation (ITC).

Appendix A.1.Calculation of orographic rainfall for the wet seas

No	Station name	elevation	total orographic rainfall (Po)	total measured rainfall (Pm)	residue	monthly average orographic rainfall	Jan_2002		Feb_2002		Mar_2002		April_2002		May_2002		Nov-02		Dec-02	
			Nov-May	Nov-May			Pm	residue	Pm	residue	Pm	residue	Pm	residue	Pm	residue	Pm	residue	Pm	residue
1	Cihanbeyli	968.7	226.41	217.50	-8.91	32.34	41.50	9.16	6.90	-25.44	26.60	-5.74	78.70	46.36	16.30	-16.04	17.20	-15.14	30.30	-2.04
2	Cumra	1013	249.01	257.80	8.79	35.57	29.80	-5.77	12.10	-23.47	22.30	-13.27	91.00	55.43	22.80	-12.77	22.10	-13.47	57.70	22.13
3	Eregli	1042	263.81	235.10	-28.71	37.69	38.90	1.21	15.80	-21.89	8.90	-28.79	77.20	39.51	15.60	-22.09	18.30	-19.39	60.40	22.71
4	Karapinar	1004	244.42	188.80	-55.62	34.92	28.30	-6.62	12.80	-22.12	7.50	-27.42	47.90	12.98	14.10	-20.82	24.90	-10.02	53.30	18.38
5	Konya	1031	258.20	221.10	-37.10	36.89	27.80	-9.09	12.90	-23.99	24.20	-12.69	70.00	33.11	22.90	-13.99	15.30	-21.59	48.00	11.11
6	Kulu	1010	247.48	234.20	-13.28	35.35	40.00	4.65	10.20	-25.15	21.90	-13.45	79.30	43.95	26.70	-8.65	28.80	-6.55	27.30	-8.05
7	Karaman	1023	254.11	296.70	42.59	36.30	40.90	4.60	30.00	-6.30	30.10	-6.20	70.70	34.40	42.70	6.40	22.20	-14.10	60.10	23.80
8	Aksaray	960.8	222.38	233.90	11.52	31.77	31.80	0.03	14.30	-17.47	16.80	-14.97	81.70	49.93	29.50	-2.27	31.90	0.13	27.90	-3.87
9	Hadim	1552	524.01	518.30	-5.71	74.86	106.50	31.64	33.40	-41.46	84.40	9.54	80.10	5.24	38.80	-36.06	62.60	-12.26	112.50	37.64
10	Ilgin	1034	259.73	327.40	67.67	37.10	60.90	23.80	27.10	-10.00	58.90	21.80	93.60	56.50	14.60	-22.50	20.00	-17.10	52.30	15.20
11	Yunak	1140	313.81	332.90	19.09	44.83	62.10	17.27	15.20	-29.63	48.50	3.67	94.90	50.07	29.80	-15.03	23.10	-21.73	59.30	14.47

Appendix A.2.Calculation of hydraulic conductivity from the pumping tests

WELL ID: Akincilar_52967

Local ID: 52967
Date: 3/7/1998
Time: 13:49

INPUT

Construction:	
Casing dia. (d_c)	0.3048 Meter
Annulus dia. (d_w)	0.4445 Meter
Screen Length (L)	60 Meter
Depths to:	
water level (DTW)	39.7 Meter
Top of Aquifer	68 Meter
Base of Aquifer	131 Meter
Annular Fill:	
across screen -- Gravel	
above screen -- Cement	
Aquifer Material -- Karst	
FLOW RATE	3888 m3/d

COMPUTED

Aquifer thickness = 63 Meter

Slope = 0.028908 Meter/log10

Input is consistent.

K = 120 Meter/Day
T = 7500 Meter²/Day

Reduced Data

Entry	Time, Date Hr:Min:Sec	Water Level Meter
1	4/19/00 13:49:00	39.70
2	4/19/00 13:50:50	41.50
3	4/19/00 13:51:45	42.00
4	4/19/00 13:52:00	42.10
5	4/19/00 13:53:00	42.15
6	4/19/00 13:55:00	42.18
7	4/19/00 13:57:00	42.20
8	4/19/00 13:59:00	42.20
9	4/19/00 14:04:00	42.20
10	4/19/00 14:09:00	42.20
11	4/19/00 14:14:00	42.20
12	4/19/00 14:19:00	42.20
13	4/19/00 16:19:00	42.20
14	4/19/00 18:19:00	42.20
15	4/19/00 22:19:00	42.20

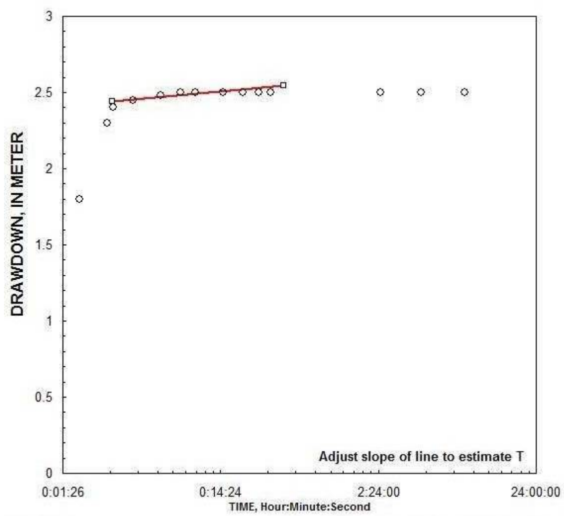

REMARKS: Cooper-Jacob analysis of single-well aquifer test

Akincilar_52967: confined aquifer, screened in miocene limestone unit

WELL ID: Akorenkisla_47890

Local ID: 47890
Date: 28/7/1996
Time: 13:49

INPUT

Construction:	
Casing dia. (d_c)	0.254 Meter
Annulus dia. (d_w)	0.3175 Meter
Screen Length (L)	61 Meter
Depths to:	
water level (DTW)	43.2 Meter
Top of Aquifer	43.2 Meter
Base of Aquifer	117 Meter
Annular Fill:	
across screen -- Gravel	
above screen -- Cement	
Aquifer Material -- Karst	
FLOW RATE	4320 m3/d

COMPUTED

Aquifer thickness = 74 Meter

Slope = 0.177518 Meter/log10

Input is consistent.

K = 18 Meter/Day
T = 1400 Meter²/Day

Reduced Data

Entry	Time, Date Hr:Min:Sec	Water Level Meter
1	4/19/00 13:49:00	40.00
2	4/19/00 13:50:50	41.10
3	4/19/00 13:51:45	41.85
4	4/19/00 13:52:00	42.30
5	4/19/00 13:53:00	42.52
6	4/19/00 13:54:00	42.61
7	4/19/00 13:55:00	42.68
8	4/19/00 13:57:00	42.74
9	4/19/00 13:59:00	42.79
10	4/19/00 14:01:00	42.83
11	4/19/00 14:03:00	42.87
12	4/19/00 14:05:00	42.91
13	4/19/00 14:07:00	42.95
14	4/19/00 14:09:00	42.99
15	4/19/00 14:11:00	43.02
16	4/19/00 14:13:00	43.03
17	4/19/00 14:15:00	43.05
18	4/19/00 14:17:00	43.06
19	4/19/00 14:19:00	43.07
20	4/19/00 14:24:00	43.09
21	4/19/00 14:29:00	43.11
22	4/19/00 15:49:00	43.12
23	4/19/00 15:54:00	43.13
24	4/19/00 15:59:00	43.14
25	4/19/00 16:04:00	43.15
26	4/19/00 16:14:00	43.17
27	4/19/00 16:24:00	43.18
28	4/19/00 16:34:00	43.19
29	4/19/00 16:44:00	43.19
30	4/19/00 16:54:00	43.19
31	4/19/00 18:54:00	43.19
32	4/19/00 20:54:00	43.19
33	4/20/00 0:54:00	43.19

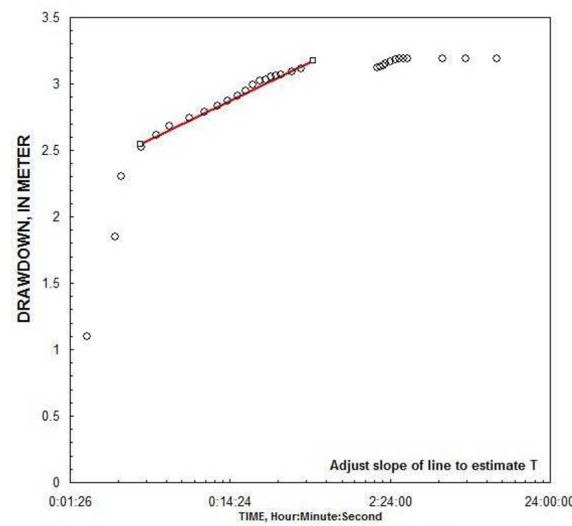

REMARKS: Cooper-Jacob analysis of single-well aquifer test

Akorenkisla_47890: confined aquifer, screened in miocene limestone unit

Appendix A.3. A photo shows two layers of the Neogene Aquifer

Appendix A.4.Hydrogeology map (1966)

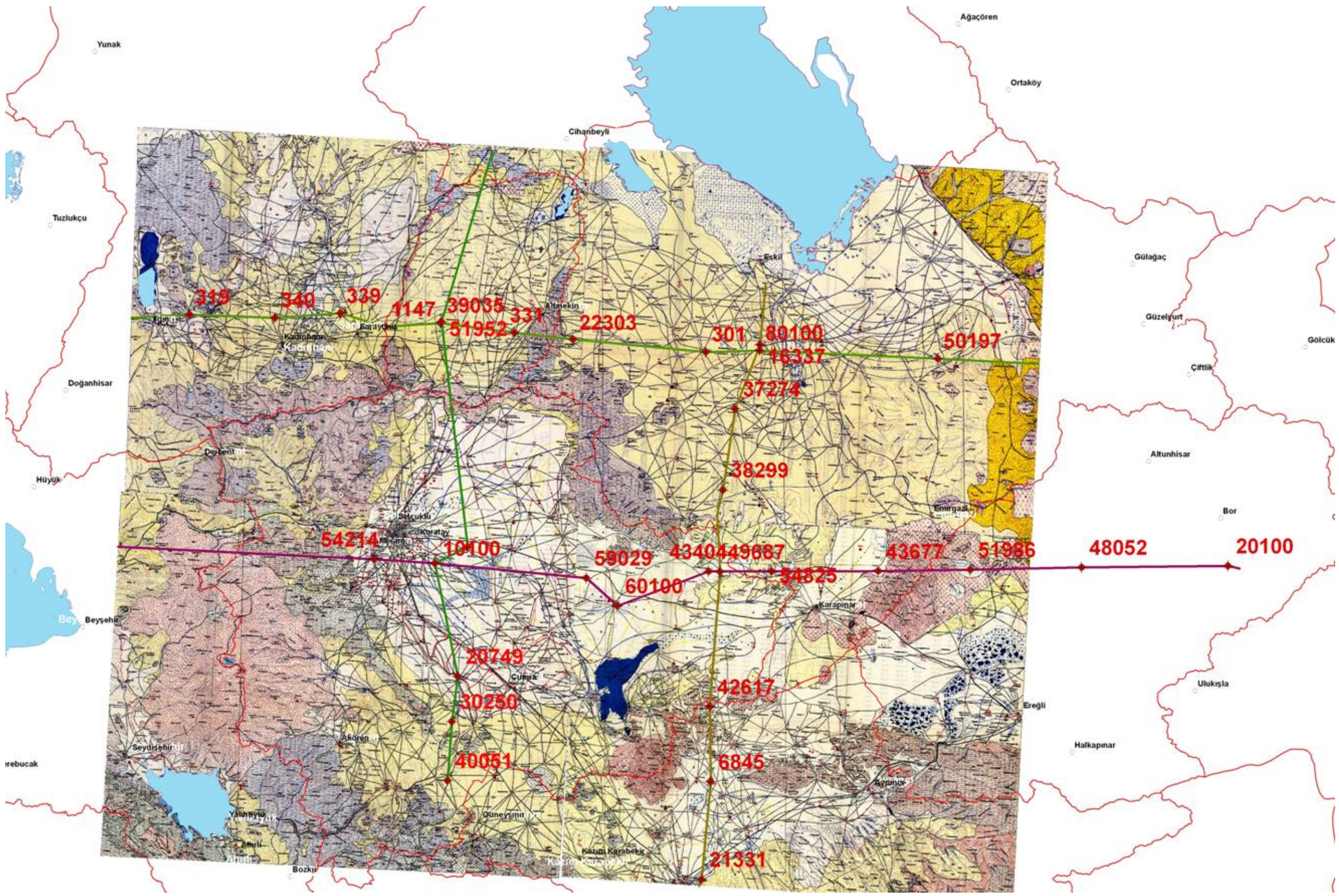

Appendix A.5.Groundwater abstraction information in zone by zone in KCB

Data on GW abstraction by Water Authority (DSI, 2010)

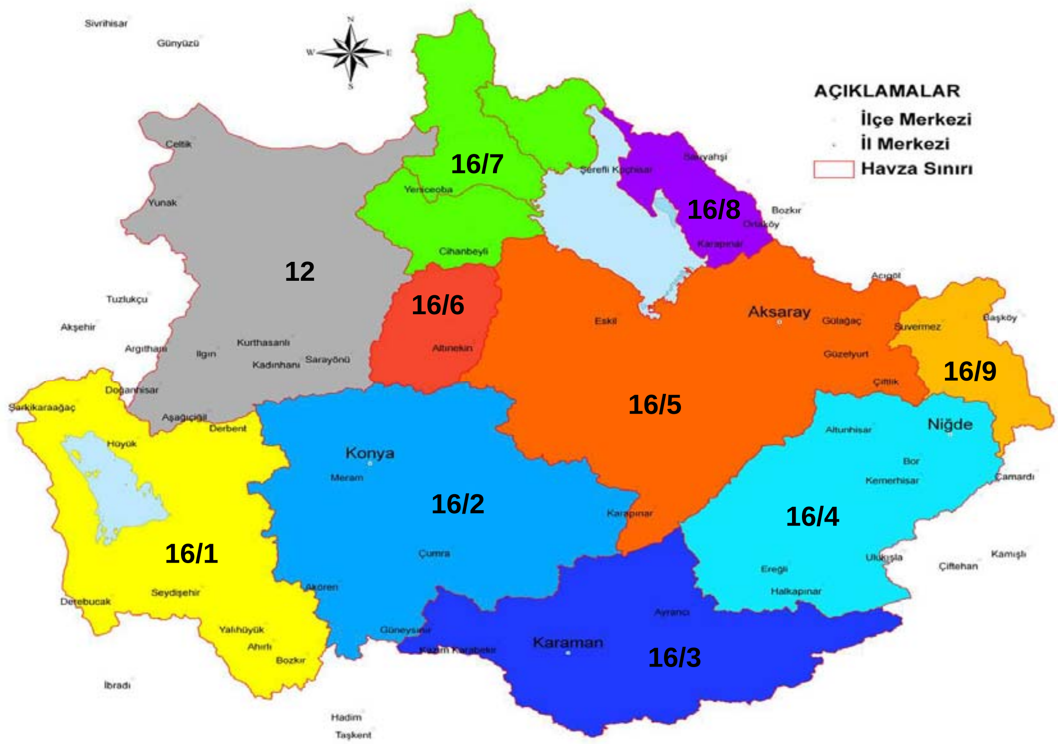

Sub basin		Potential reserve	GW abstraction (hm³, or MCM)						BALANCE
			Agriculture				Drinking water	TOTAL	
			Coop. wells	Registered wells	Unregis. wells	Additional			
16/2	Konya-Çumra	444	364	137	428	53	100	1082	-638
16/4	Ereğli-Bor	443	118	48	279	25	10	480	-37
16/5	Sultanhanı-Obruk - Karapınar	435	186	275	306	31	20	818	-383
16/6	Altınekin	74	11	86	38	-	5	140	-66
16/7	Kulu-Cihanbeyli-Y.oba	70	8	53	73	-	5	139	-69
15-17-18		50	-	6	44	-	-	50	
TOPLAM		2407	1000	875	1625	125	178	3803	-1396